

This work was written as part of one of the author's official duties as an Employee of the United States Government and is therefore a work of the United States Government. In accordance with 17 U.S.C. 105, no copyright protection is available for such works under U.S. Law.

Public Domain Mark 1.0

<https://creativecommons.org/publicdomain/mark/1.0/>

Access to this work was provided by the University of Maryland, Baltimore County (UMBC) ScholarWorks@UMBC digital repository on the Maryland Shared Open Access (MD-SOAR) platform.

**Please provide feedback**

Please support the ScholarWorks@UMBC repository by emailing [scholarworks-group@umbc.edu](mailto:scholarworks-group@umbc.edu) and telling us what having access to this work means to you and why it's important to you. Thank you.

# Spatial and temporal variability of column-integrated aerosol optical properties in the southern Arabian Gulf and United Arab Emirates in summer

T. F. Eck,<sup>1,2</sup> B. N. Holben,<sup>3</sup> J. S. Reid,<sup>4</sup> A. Sinyuk,<sup>5,2</sup> O. Dubovik,<sup>6</sup> A. Smirnov,<sup>1,2</sup> D. Giles,<sup>5,2</sup> N. T. O'Neill,<sup>7</sup> S.-C. Tsay,<sup>3</sup> Q. Ji,<sup>8,2</sup> A. Al Mandoos,<sup>9</sup> M. Ramzan Khan,<sup>9</sup> E. A. Reid,<sup>4</sup> J. S. Schafer,<sup>5,2</sup> M. Sorokine,<sup>5,2</sup> W. Newcomb,<sup>5,2</sup> and I. Slutsker<sup>5,2</sup>

Received 10 May 2007; revised 3 August 2007; accepted 20 September 2007; published 15 January 2008.

[1] A mesoscale network of 14 AERONET Sun photometers was established in the UAE and adjacent Arabian Gulf from August through September 2004 as a component of the United Arab Emirates Unified Aerosol Experiment (UAE<sup>2</sup>). These measurements allowed for spatial, temporal and spectral characterization of the complex aerosol mixtures present in this environment where coarse mode desert dust aerosols often mix with fine mode pollution aerosols largely produced by the petroleum industry. Aerosol loading was relatively high with 2-month averages of aerosol optical depth (AOD) at 500 nm ( $\tau_{a500}$ ) ranging from 0.40 to 0.53. A higher fine mode fraction of AOD was observed over Arabian Gulf island sites with Angstrom exponent at 440–870 nm ( $\alpha_{440-870}$ ) of 0.77 as compared to an average of 0.64 over coastal sites and 0.50–0.57 at inland desert sites. During pollution events with  $\alpha_{440-870} > 1$  the retrieved fine mode radius was larger over an island site than a desert site probably because of hygroscopic growth over the humid marine environment. For these same pollution cases, single scattering albedo ( $\omega_0$ ) at all wavelengths was  $\sim 0.03$  higher (less absorption) over the marine environment than over the desert, also consistent with aerosol humidification growth. At an inland desert location, the  $\omega_0$  at 440 nm remained relatively constant as Angstrom exponent varied since the fine mode pollution and coarse mode dust were both strong absorbers at short wavelengths. However, at longer wavelengths (675–1020 nm) the dust was much less absorbing than the pollution resulting in dynamic  $\omega_0$  as a function of  $\alpha_{440-870}$ .

**Citation:** Eck, T. F., et al. (2008), Spatial and temporal variability of column-integrated aerosol optical properties in the southern Arabian Gulf and United Arab Emirates in summer, *J. Geophys. Res.*, 113, D01204, doi:10.1029/2007JD008944.

## 1. Introduction

[2] In the summer of 2004 the UAE Unified Aerosol Experiment (UAE<sup>2</sup>) field campaign was conducted in the United Arab Emirates and over the adjacent Arabian Gulf and Gulf of Oman waters (J. S. Reid et al., Dynamics of southwest Asian dust particle size characteristics with

implications for global dust research, submitted to *Journal of Geophysical Research*, 2007, hereinafter referred to as Reid et al., submitted manuscript, 2007a). The focus areas of this field campaign included the characterization of fundamental physical and optical properties of atmospheric aerosol particles, the interaction of the regional/local meteorology with the aerosol radiative impacts, and the remote sensing of heterogeneous aerosol properties over the water and bright desert surfaces. Over sixty scientists and engineers from several countries participated in ground-based and airborne data collection and analysis.

[3] The aerosol environment in this region is extraordinarily complex. The geographical location of the UAE includes strong regional desert dust sources of predominantly coarse mode-size particles and complex shape, as well as strong fine mode pollution particle sources from petroleum extraction and processing facilities. This variability of atmospheric particle type, size, and shape in conjunction with highly variable regional meteorology results in some days that are dominated by large particle desert dust, some dominated by fine particle pollution, and many days

<sup>1</sup>Goddard Earth Sciences and Technology Center, University of Maryland, Baltimore County, Baltimore, Maryland, USA.

<sup>2</sup>Also at NASA Goddard Space Flight Center, Greenbelt, Maryland, USA.

<sup>3</sup>NASA Goddard Space Flight Center, Greenbelt, Maryland, USA.

<sup>4</sup>Naval Research Laboratory, Monterey, California, USA.

<sup>5</sup>Science Systems and Applications, Inc., Lanham, Maryland, USA.

<sup>6</sup>Laboratoire d'Optique Atmosphérique, Université de Lille, Villeneuve d'Ascq, France.

<sup>7</sup>CARTEL, Université de Sherbrooke, Sherbrooke, Quebec, Canada.

<sup>8</sup>Earth System Science Interdisciplinary Center, University of Maryland, College Park, Maryland, USA.

<sup>9</sup>Department of Atmospheric Studies, Ministry of Presidential Affairs, Abu Dhabi, United Arab Emirates.

that are a mixture of aerosol types. Additionally, the high spectral reflectance of most arid land surfaces in the region results in difficulty in remote sensing of aerosol optical properties from satellites.

[4] A major component of the UAE<sup>2</sup> field campaign was the establishment of 14 Aerosol Robotic Network (AERONET) Sun photometer sites in various environments including Arabian Gulf islands, coastal locations, inland deserts, and a mountain ridge top. This measurement campaign provided the highest density mesoscale network of sites ever established by AERONET, and allowed for regional study of the temporal and spatial variation of effective total column integrated optical properties in addition to more rigorous than usual characterization of both satellite and ground based remote sensing retrievals. Here we investigate the spatial distribution and temporal dynamics of the total column atmospheric aerosol optical depth (AOD), and retrieved aerosol size distributions and single scattering albedo. AERONET retrievals yield the total column radiatively effective size distributions and single scattering albedos. This study attempts to quantify the dynamics of aerosol optical properties in the late summer season in the UAE. Information on the variability of these spectrally variable optical parameters is presented to aid in the refinement and validation of remote sensing retrievals of aerosol optical depth and properties and in determining the potential climatic effects of aerosol perturbations to the regional radiation budget. Additionally, by using the prevalence of open desert, coastal, and open water sites and range of aerosol types and mixtures we examine the characteristics of the new AERONET version 2 retrievals.

## 2. Instrumentation, Study Sites, and Techniques

### 2.1. AERONET Instrumentation

[5] The CIMEL Electronique CE-318 Sun-sky radiometer measurements reported in this paper were made with instruments that are a part of the AERONET global network. These instruments are described in detail in the work of *Holben et al.* [1998], however a brief description will be given here. The automatic tracking Sun and sky scanning radiometers made direct Sun measurements with a 1.2° full field of view every 15 min at 340, 380, 440, 500, 675, 870, 940, and 1020 nm (nominal wavelengths). Additionally 4 sites (Dalma, Dhadnah, SMART and MAARCO) had the new extended wavelength version of the CIMEL with the 1640-nm channel added to the 8 standard wavelengths (we do not analyze the 1640-nm data in this paper as this is the topic of another investigation [*O'Neill et al.*, 2008]). For the SMART\_POL site the polarized version of the CIMEL made measurements at 440, 675, 870, 940, and 1020 nm, in addition to three polarized channels at 870 nm (the polarized channels were also not analyzed in this study). The direct Sun measurements take ~8 seconds to scan all 8 wavelengths, with a motor driven filter wheel positioning each filter in front of the detector. These solar extinction measurements are then used to compute aerosol optical depth at each wavelength except for the 940-nm channel, which is used to retrieve total columnar (or precipitable) water vapor in centimeters. The filters utilized in these instruments were ion assisted deposition interference filters with bandpass (full width at half maximum) of 10 nm, except

for the 340- and 380-nm channels at 2 nm. Calibration of field instruments was performed by a transfer of calibration from reference instruments that were calibrated by the Langley plot technique at Mauna Loa Observatory (MLO), Hawaii. The intercalibration of field instruments was performed both predeployment and postdeployment at Goddard Space Flight Center (GSFC) and a linear change in calibration with time was assumed in the interpolation between the two calibrations. The uncertainty, due primarily to calibration uncertainty is ~0.010–0.021 in computed  $\tau_a$  for field instruments (which is spectrally dependent with the higher errors in the UV; *Eck et al.* [1999]). *Schmid et al.* [1999] compared  $\tau_a$  values derived from 4 different solar radiometers (including an AERONET Sun-sky radiometer) operating simultaneously together in a field experiment and found that the  $\tau_a$  values from 380 to 1020 nm agreed to within 0.015 (rms), which is similar to our estimated level of uncertainty in  $\tau_a$  retrieval for field instruments. The spectral aerosol optical depth data have been screened for clouds following the methodology of *Smirnov et al.* [2000], which relies on the greater temporal variance of cloud optical depth versus aerosol optical depth. The sky radiances measured by the Sun/sky radiometers are calibrated versus the 2-m integrating sphere at the NASA Goddard Space Flight Center, to an absolute accuracy of ~5% or less.

### 2.2. Study Region and Sites

[6] Figure 1 presents a map of the UAE and Arabian Gulf showing the 14 AERONET sites that were deployed for the UAE<sup>2</sup> field campaign. We analyzed data from 12 of these sites in the current study, excluding the Abu Al Bukhoosh site since it was only established on 20 September 2004, toward the end of the campaign period, and also excluding the Dhabhi site since there were multiple changes in instruments (and some instrument problems). The distribution of analyzed sites covers all of the major environments in the region including Gulf islands (Dalma and Sir Bu Nuair), coastal sites (Al Qlaa, MAARCO, Umm Al Quwain, and Dhadnah), inland desert sites (Mezaira, Hamim, and SMART), coastal plain/inland sites (Saih Salam and Al Khaznah), and a mountain ridge site (Jabal Hafeet). This dense distribution of sites is unique in the history of AERONET and it allows for the study of differences in aerosol properties owing to relative humidity differences (very humid over the Gulf versus very dry over the desert), vertical distribution of aerosol (mountain site at Jabal Hafeet versus nearby desert site, SMART at Al Ain), and differences between coastal sites located on the Arabian Gulf versus the Gulf of Oman (Umm Al Quwain versus Dhadnah). In order to help perform primary validation of new over-desert satellite optical depth algorithms (such as Deep Blue (N. C. Hsu et al., Deep blue characterization of dust and pollution aerosols during the UAE2 experiment, submitted to *Journal of Geophysical Research*, 2007)), sites were also chosen on the basis of regional surface albedo, with sites bordering dramatic shifts in surface properties receiving a high priority for data collection and analysis (such as Hamim and Mezera).

[7] Two placements during the UAE campaign were associated with mobile laboratory super sites: the Naval Research Laboratory (NRL) Mobile Atmospheric Aerosols and Radiation Characterization Observatory (MAARCO

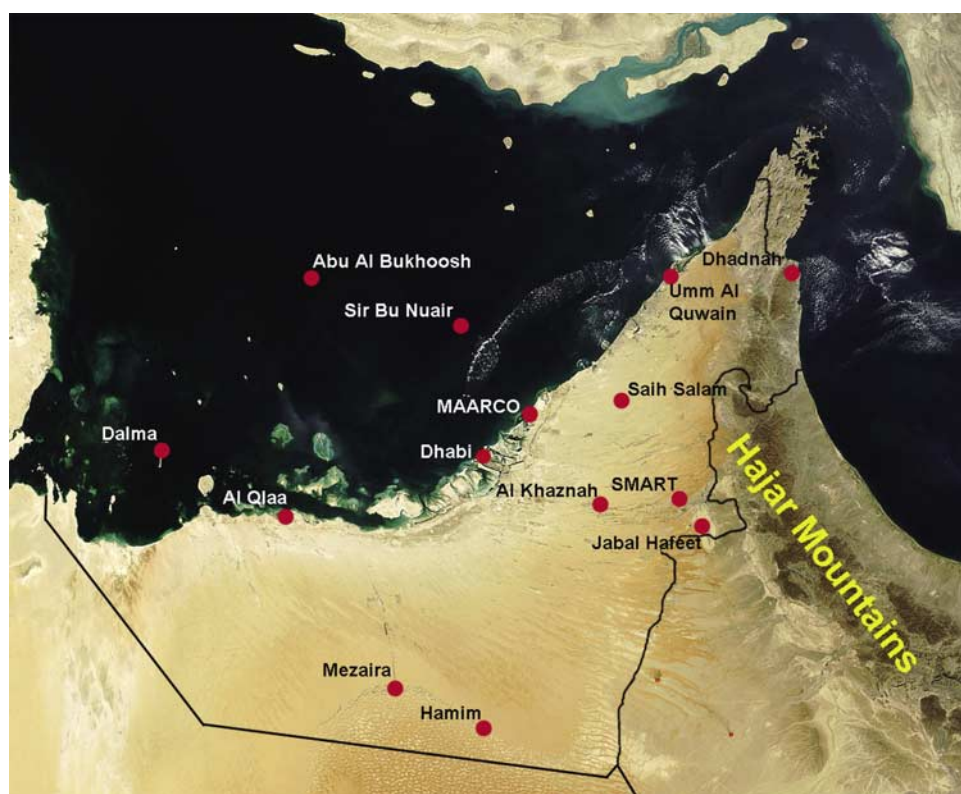


**Figure 1.** Location of AERONET sites in the United Arab Emirates and southern Arabian Gulf during the UAE<sup>2</sup> field campaign during the summer of 2004.

(J. S. Reid et al., Observations of summertime atmospheric thermodynamic and aerosol profiles of the southern Arabian Gulf, submitted to *Journal of Geophysical Research*, 2007, hereinafter referred to as Reid et al., submitted manuscript, 2007b)); and the NASA Goddard SFC Surface-Sensing Measurements for Atmospheric Radiative Transfer (SMART; <http://smart-commit.gsfc.nasa.gov>). The MAARCO site was located on the coast ~60 km northeast of Abu Dhabi and housed an extensive set of instruments for meteorological measurements, in situ aerosol sampling, and aerosol remote sensing. The SMART trailer, with a complete set of surface based radiation and remote sensing instrumentation, was established at the inland desert site located at the Al Ain airport.

### 2.3. Inversion Methodology

[8] The CIMEL sky radiance measurements in the almucantar geometry (fixed elevation angle equal to solar elevation and a full 360° azimuthal sweep) at 440, 675, 870, and 1020 nm (nominal wavelengths) in conjunction with the direct Sun measured  $\tau_a$  at these same wavelengths were used to retrieve optical equivalent aerosol size distributions and refractive indices. Using this microphysical information the spectral dependence of single scattering albedo ( $\omega_0$ ) is calculated. The algorithm of Dubovik and King [2000] with enhancements detailed in the work of Dubovik et al. [2006] was utilized in these retrievals, known as version 2 AERONET retrievals. Level 2 quality assured retrievals [Holben et al., 2006] are presented in this paper. In the version 2 algorithm, particle shape is partitioned into two components: spherical and nonspherical. The spherical component is

modeled as an ensemble of polydisperse homogeneous spheres, while the nonspherical component is modeled as a mixture of polydisperse randomly oriented homogeneous spheroids with a fixed aspect ratio distribution. The spheroid aspect ratio distribution utilized is the one obtained from fitting [see Dubovik et al., 2006] of the phase matrix measurements of feldspar by Volten et al. [2001], and it is used in all AERONET retrievals (regardless of the mineral type of the dust). As discussed in the work of Dubovik et al. [2006], this model is capable of reproducing the main features of nonspherical dust light scattering properties required for the fitting of observations. In addition, the fitting error of this algorithm to AERONET measurements of dust is small (comparable to measurement accuracy), indicating that the model works rather well in all cases. Use of only one model in AERONET dust retrievals is supported by the fact that AERONET radiometric measurements are not sensitive to details of the aspect ratio distribution [see Dubovik et al., 2006]. For example, as discussed by Dubovik et al. [2006], simple mixtures of spheroids with relatively constant aspect ratios ranging from 1.5 to 3 are able to reproduce the main features of nonspherical dust scattering. Information on the morphology of ambient mineral dust is very difficult to collect and these measurements were not made during the UAE<sup>2</sup> campaign. The version 2 AERONET algorithm determines the percentage of spherical particles required to give the best fit to the measured spectral sky radiance angular distribution.

[9] Another improvement made in the version 2 almucantar retrievals is the specification of more accurate surface reflectance as an input boundary condition to the retrieval.



**Table 1.** Average Surface Albedo Computed From AERONET Version 2 Bidirectional Reflectance Distribution Function Compared to Albedo Assumed for All Sites in Version 1<sup>a</sup>

Site Name	Albedo			
	440 nm	675 nm	675 nm	1020 nm
Sir Bu Nuair	0.11	0.12	0.12	0.13
Hamim	0.14	0.47	0.59	0.62
Al Qlaa	0.16	0.29	0.33	0.34
Version 1, all sites	0.03	0.06	0.20	0.20

<sup>a</sup>Average surface albedo have a solar zenith angle range of 50 to 77.

Large errors in prescribed surface reflectance can affect the accuracy of retrieved aerosol parameters including single scattering albedo [Sinyuk *et al.*, 2007]. In version 1 the reflectance was assumed to be Lambertian and invariant geographically, with reflectance values of 0.03, 0.06, 0.20, and 0.20 for the 440-, 675-, 870-, and 1020-nm wavelengths, respectively. Bright soil and sand surfaces of the arid environments in the UAE have much higher spectral reflectance (and consequently result in greater sky brightness) than the values assumed in version 1 retrievals. In version 2, bidirectional reflectance distribution function (BRDF) models are utilized that allow for dynamic reflectance as a function of solar zenith angle over land and water. Over the ocean, the Cox and Munk [1954] model approximates the water BRDF as a function of wind speed (wind speed data are from NCEP/NCAR Reanalysis; Kalnay *et al.* [1996]) and over the land the Li-Ross model of Lucht and Roujean [2000] is applied. The land BRDF parameters are adopted from MODIS generic ecosystem type models and mixed by the ecosystem map of Moody *et al.* [2005]. Geographically and seasonally (16-day interval) varying surface albedo estimates from Moody *et al.* [2005], on the basis of MODIS atmospherically corrected data, were used to vary the magnitude of the BRDF values. The MODIS albedo data from a 5 km radius centered on each site are averaged. In Table 1 the spectral albedo values computed from version 2 BRDF for the solar zenith angle range 50° to 77° are given for an inland sandy desert site (Hamim), an Arabian Gulf island site (Sir Bu Nuair; only ~15% land), and a coastal site (Al Qlaa, ~50% land). Obviously, the table shows significant variation in surface albedo in the study region and also significant departure from the version 1 assumption for all sites.

[10] Almucantar sky radiance measurements were made at optical air masses of 4, 3, 2, and 1.7 in the morning and afternoon, and once per hour in between. In order to ensure sky radiance data over a wide range of scattering angles, only almucantar scans at solar zenith angles greater than 50° are analyzed and presented here. To eliminate cloud contamination from the almucantar directional sky radiance data we require the radiances to be symmetrical on both sides of the Sun at equal scattering angles. The stable performance of the inversion algorithm was illustrated in sensitivity studies performed by Dubovik *et al.* [2000] where the perturbations of the inversion resulting from random errors, possible instrument offsets and known uncertainties in the atmospheric radiation model were analyzed. Retrieval tests using known size distributions demonstrated successful retrievals of mode radii and the

relative magnitude of modes for various types of bimodal size distributions such as those dominated by a submicron accumulation mode or distributions dominated by coarse mode aerosols.

### 3. Results and Discussion

#### 3.1. Spatial, Temporal, and Spectral Variability of AOD

##### 3.1.1. Temporal and Spatial Variability of Daily Average AOD and Angstrom Exponent

[11] A time series of daily average AOD at 500 nm from 9 August through 2 October 2004 for four AERONET station sites (Sir Bu Nuair, Umm Al Quwain, Saih Salam, and SMART) in the UAE is shown in Figure 2a. These sites

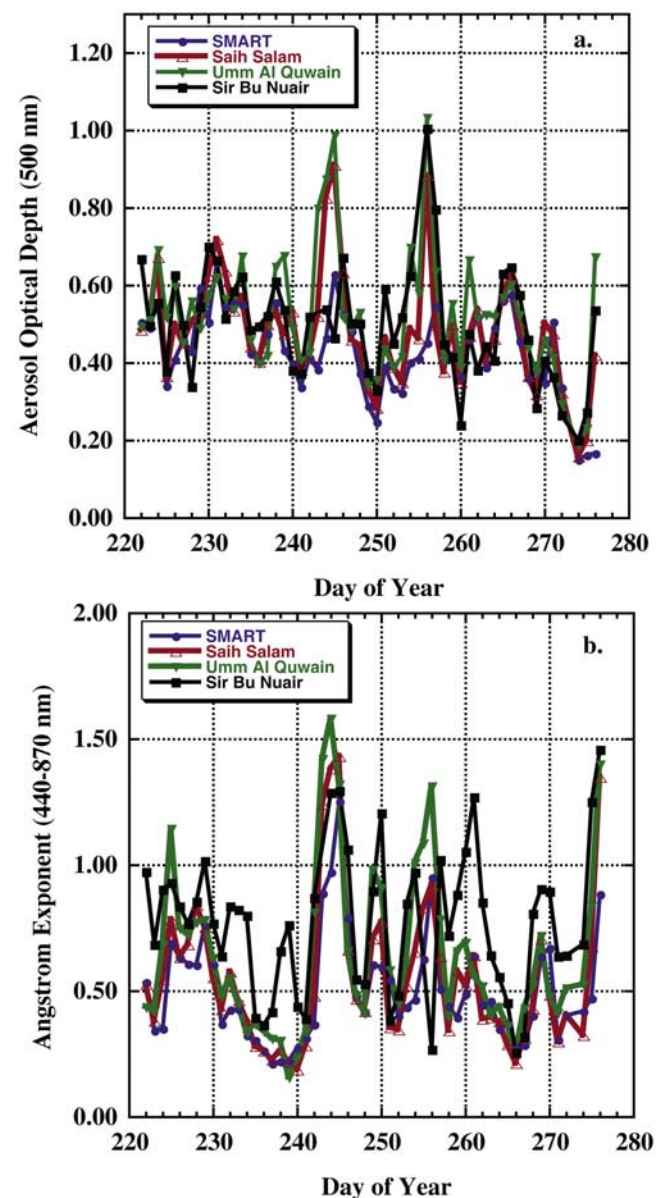


**Figure 2.** Time series of daily averages of aerosol optical depth (500 nm) and Angstrom exponent (440–870 nm), from 9 August through 2 October 2004, for three sites in the United Arab Emirates and one in the adjacent Arabian Gulf.

**Table 2.** Average Aerosol Optical Depth, Angstrom Exponent, and Columnar Water Vapor for 9 August to 2 October 2004

Site Name	Location	Aerosol Optical Depth, 500 nm	Angstrom Exponent, 440/870 nm	Water Vapor, cm
Dalma	Gulf island	0.44	0.77	2.48
Sir Bu Nuair	Gulf island	0.49	0.77	3.09
MAARCO <sup>a</sup>	coast	0.48	0.64	2.75
Umm Al Quwain	coast	0.53	0.64	3.31
Saih Salam	coastal plain	0.49	0.55	2.77
Mezaira	inland desert	0.40	0.57	2.32
Hamim	inland desert	0.41	0.57	2.47
SMART <sup>b</sup>	inland desert	0.43	0.50	2.44

<sup>a</sup>MAARCO, Mobile Atmospheric Aerosols and Radiation Characterization Observatory.

<sup>b</sup>SMART, Surface-Sensing Measurements for Atmospheric Radiative Transfer.

are a representative sample over various environments, including, respectively, an Arabian Gulf island site, a coastal site, a site on the coastal plain, and an inland site. It is noted that the 500-nm AOD is typically quite high at all sites in this season, exceeding  $\sim 0.4$  on most days with maximum values of  $\sim 1.0$  and minimum of  $\sim 0.15$ . The temporal variability patterns are similar for these sites on most days suggesting that regional-scale aerosol variation often dominates over local effects. Table 2 shows averages of the AOD (500 nm), Angstrom exponent (440–870 nm), and total columnar water vapor for the entire time interval for eight sites in the UAE. For six of the eight sites in Table 2 there are 55 daily averages (no missing days), while the other 2 sites have 53 and 54 daily averages that are utilized to compute the 9 August to 2 October mean. This high data collection rate results from the very low incidence of cloud cover in much of the UAE during the summer season. Other sites are not included in Table 2 since there were too many missing days over this time interval, thus negating direct comparisons. The  $\sim 2$ -month average AOD for these eight sites ranges from 0.40 to 0.53, with all inland desert sites having lower AOD (0.40 to 0.43), while most island and coastal sites have higher values (0.48 to 0.53). However, the island site of Dalma has relatively low AOD (0.44) indicating that the relative location to the Arabian Gulf is not in itself an accurate predictor of aerosol loading. Location relative to upwind aerosol sources coupled with the sometimes complicated mesoscale flows are likely key reasons for regional variability. It is interesting that the total columnar water vapor over Dalma is similar to that over the inland desert sites, further suggesting complex variation in regional-scale circulation. The proximity of Dalma to the Qatar peninsula may influence the local boundary layer circulation.

[12] The time series of the daily average Angstrom wavelength exponent (computed from 440- to 870-nm AOD data) for the same sites and dates is shown in Figure 2b. It is noted in this figure that the Angstrom exponent is quite variable, ranging from  $\sim 0.2$  to  $\sim 1.6$ , as a result of some days being dominated by strong desert dust events and some days where pollution aerosol is predominant although most days exhibit a mixture of aerosol types.

At these four UAE sites, the Angstrom exponent averages 0.77 for the Gulf island site of Sir Bu Nuair, 0.64 for the coastal site of Umm Al Quwain, and 0.55 and 0.50 at the inland desert sites of Saih Salam and SMART, respectively. Therefore the higher Angstrom exponent values for the Gulf island and coastal sites indicate that fine mode pollution particles are present in greater concentrations there than at inland desert sites. Table 2 shows a strong relationship between geographical location and the average Angstrom exponents, with both Gulf island sites having  $\alpha = 0.77$ , both sites on the coast having 0.64 and inland desert sites ranging from 0.50 to 0.57. Higher Angstrom exponents at sites in or bordering the Arabian Gulf are likely due to the sources of fine mode particle pollution originating from petroleum industry operations at offshore platforms, on islands, and on the coast. These fine mode aerosol particles are dominated by sulfates (K. E. Ross et al., Fine mode aerosol particles in the southern Arabian Gulf and United Arab Emirates, submitted to *Journal of Geophysical Research*, 2007, hereinafter referred to as Ross et al., submitted manuscript, 2007) that are very hygroscopic; therefore they grow in size in high-humidity environments, which thereby increases the fine mode scattering optical depth. The slightly higher  $\alpha$  at Hamim and Mezaira compared to the SMART site may result from the emissions of a large oil processing complex located approximately midway between the Gulf coast and the Hamim and Mezaira sites.

### 3.1.2. Diurnal Variability of AOD and Angstrom Exponent

[13] As discussed in the work of R. E. Eager et al. (A climatological study of the sea and land breezes in the Arabian Gulf Region, submitted to *Journal of Geophysical Research*, 2007, hereinafter referred to as Eager et al., submitted manuscript, 2007) the southern Arabian Gulf is strongly influenced by regional sea and land breeze circulations. The impact of these circulations can be seen in Figure 3, where the mean diurnal variability of AOD and Angstrom exponent expressed as the departure from the daily mean versus the local time of day is presented. At each site the means for each day are computed and then the absolute departure from that is computed for each observation, and averaged in hourly bins (similar to Smirnov et al. [2002a]). The departures from daily mean for each hour are then averaged over an approximately 2 month period, August through September for most sites, although for Al Qlaa the time period was 24 June to 24 August since the instrument was removed from the site on 25 August. For most sites the departures from the daily mean do not exceed 0.02 for most hours (change of  $<5\%$ ), and with no strong trend over the daily cycle.

[14] Two sites that do show similar coherent diurnal trends are MAARCO and Sir Bu Nuair. At both of these locations the AOD is maximum in the early morning and then it decreases slowly at first through the morning and midday and then more rapidly in the afternoon. The average minimum to maximum range of AOD at these sites is  $\sim 0.07$ . This pattern is explained by the diurnal land-sea breeze circulations (Eager et al., submitted manuscript, 2007). During morning hours the coastal UAE experiences offshore flow. Dust generated from the previous day is carried out toward the coast and the Gulf, increasing AOD and decreasing the Angstrom exponent. By midday, flows



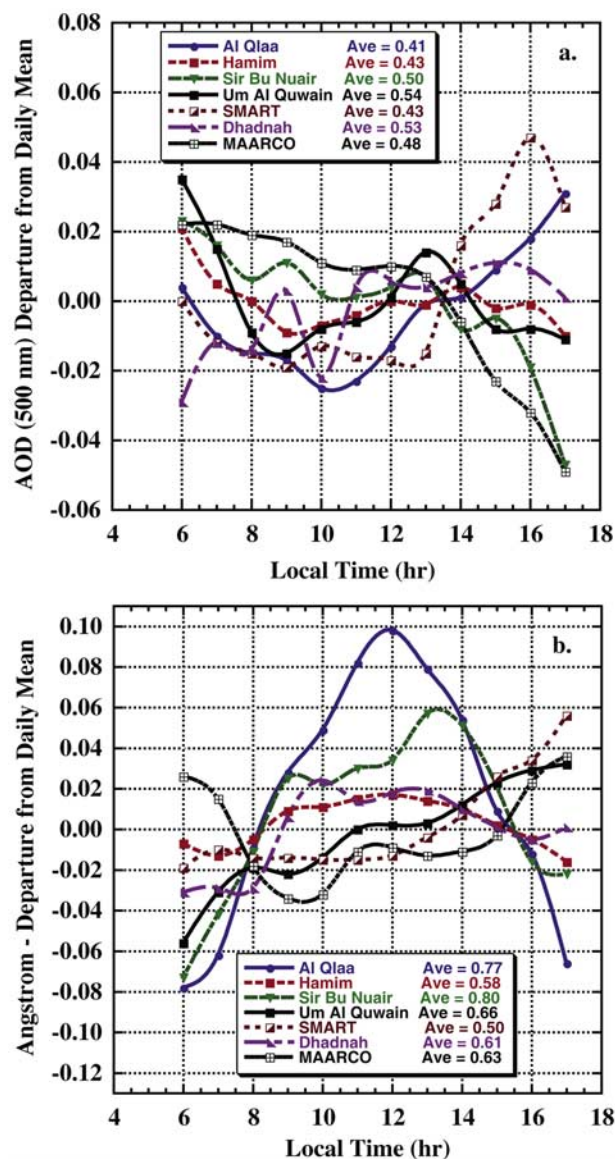


**Figure 3.** Mean diurnal variability of aerosol optical depth (AOD; 500 nm) and Angstrom exponent (440–870 nm) expressed as departures from the daily mean versus hour of the day.

reverse to onshore, with a lesser burden of dust (and consequently AOD) and occasional increases of fine mode particles from offshore petroleum operations.

[15] Another site that exhibits a similarly large range of average AOD over the diurnal cycle is the SMART site with a minimum in mid morning through midday and a maximum in late afternoon. This scenario is also explained by the land and sea-breeze circulations. The sea breeze front usually arrives at  $\sim 1000$ – $1100$  LST bringing with it a  $\sim 2$ – $3 \text{ m s}^{-1}$  increase in wind speed. These sea breeze winds often reached the interior desert by  $1400$ – $1500$  LST and frequently moved as far inland as the SMART site and sometimes to the Hamim site, bringing with them dust produced over the UAE desert. A second phenomenon, the haboob, or strong surface winds (a result of thunderstorm outflow) was also frequently observed over the

interior desert sites during the mission [Miller *et al.*, 2008]. Thunderstorms are prevalent in the afternoon over the Al Hajar Mountains and haboob events are commonplace, particularly at the SMART site. Because these thunderstorms form to the east of the SMART site, and the afternoon Sun was in the west, clouds did not usually obscure the Sun photometer view of the solar disc.

[16] Depending on where exactly an AERONET site was located, the mesoscale circulations of the southern Arabian Gulf region left its signature on the heterogeneous aerosol mixture. The diurnal patterns of Angstrom exponent vary considerably for sites in similar environments. For example the diurnal cycle of  $\alpha$  is very large at Al Qlao with a range of 0.18 (average is 0.77) and a clear pattern of maximum at local noon and minima in the early morning and late afternoon. This pattern contrasts with the diurnal cycle at MAARCO, also a coastal site, which shows a much smaller range,  $\sim 0.07$ , and with nearly the opposite diurnal pattern. The inland desert site of Hamim had the smallest diurnal range of  $\alpha$  ( $\sim 0.03$ ), and this site also had a small diurnal range in AOD, also  $\sim 0.03$ . This interior desert site was rarely influenced by the sea breeze or by haboobs.

### 3.1.3. Regional Comparison: Arabian Gulf Coast Versus Gulf of Oman Coast

[17] One scientific objective of the UAE2 mission was to understand if aerosol properties transit the Al Hajar mountains in the vicinity of the Strait of Hormuz. Typically, the Strait of Hormuz is a convergence zone of southwesterly winds traveling along the western UAE coast and easterly winds passing through the Gulf of Oman. In particular, do the optical depths and Angstrom exponents share similar characteristics, or are there different aerosol properties on the Gulf of Oman and Arabian Gulf? A comparison of the AOD and Angstrom exponents at Dhadnah, located near the coast of the Gulf of Oman, with Umm Al Quwain near the Arabian Gulf coast are shown in Figure 4. These two sites are nearly at the same latitude,  $25.513^\circ\text{N}$  and  $25.533^\circ\text{N}$  ( $\sim 2 \text{ km}$  different in north–south direction) and both are located at relatively low altitude ( $< 82 \text{ m}$ ) but are separated  $\sim 70 \text{ km}$  in the east–west direction with a mountain range between them. Daily averages are computed only from observations that are also matched in time by 5 min or less between the two sites. For the period 29 June to 13 October 2004, there were 81 days when observations were date and time matched. Scatterplots of daily average matched AOD and Angstrom exponents in Figures 4a and 4b show that there is relatively high correlation in AOD between the sites ( $\sim 61\%$  of the variance explained) and even higher correlation in Angstrom exponent ( $\sim 74\%$  of the variance explained). This suggests that on most of the days in summer 2004 the mountain range in the northern UAE between these sites did not act as a separation barrier for aerosol type, as the aerosol concentrations and size mixture were similar on both sides of the mountains.

### 3.1.4. Regional Comparison: Mountain Ridge Top Versus Base Altitude

[18] Measurements made at the top of the mountain ridge at Jabal Hafeet at  $1059\text{-m}$  altitude were compared to measurements made at the SMART site in Al Ain at  $250\text{-m}$  altitude in order to investigate the vertical partitioning of AOD in the region, for the time interval 11 August to 3 October 2004 (Figure 5). The sites were only  $\sim 28 \text{ km}$  apart

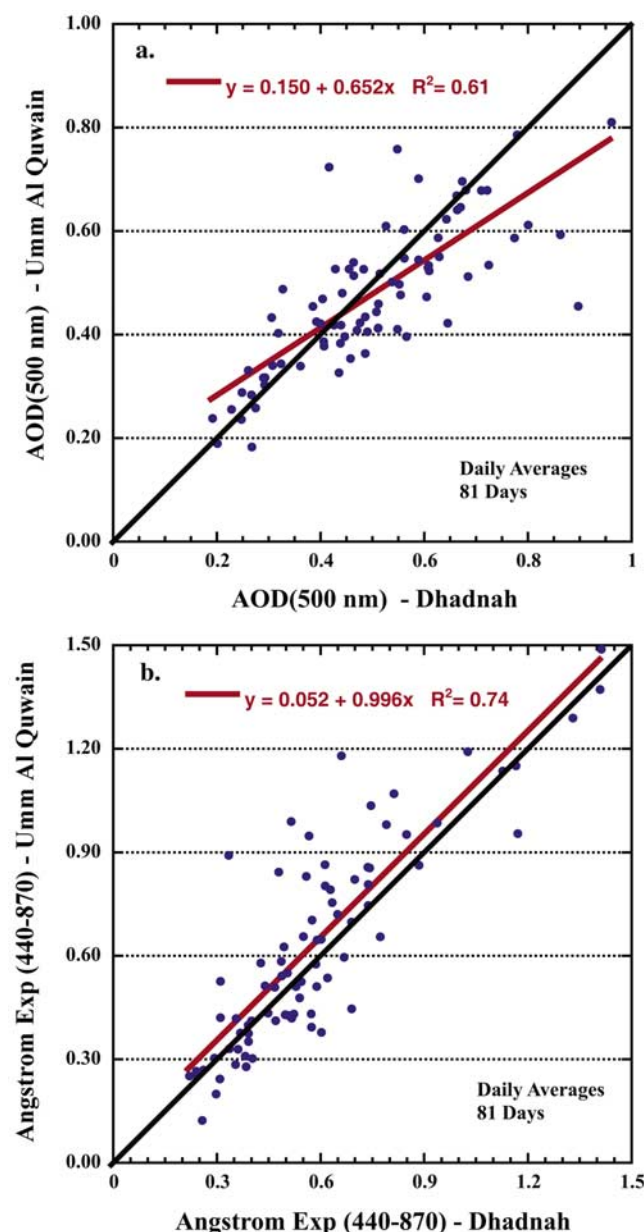


**Figure 4.** (a) Relationship between aerosol optical depth (AOD; 500 nm) at Umm Al Quwain versus Dhadnah, two sites separated by a mountain range, at the same latitude but  $\sim 70$  km apart in east–west direction. (b) Same as in Figure 4b, but for the Angstrom exponent (440–870 nm).

in horizontal distance but differed in altitude by about 800 m. The AOD (500 nm) at these sites were very highly correlated ( $r^2 = 0.85$ ), as expected from their relatively close horizontal proximity. The 500-nm AOD at Jabal Hafeet averaged 75% of the value measured at the SMART site with daily average ratios ranging from 51% to 91% (Figure 5). Therefore an average of  $\sim 25\%$  of the total column aerosol AOD at the SMART site was attributed to the lowest 800 m above ground level during the measurement period. In the interior desert, afternoon boundary layer heights reached 3 km (Reid et al., submitted manuscript, 2007a). Above 3 km additional aerosol layers exist from

long-range transport from Europe, Africa, and southwest Asia (Reid et al., submitted manuscript, 2007a).

[19] The altitude difference between the desert floor and Jabal Hafeet is similar to the altitude difference across the mountain range separating the low-altitude sites of Dhadnah and Umm Al Quwain for a  $\sim 70$  km north–south saddle between the sites (although farther to the north and south some individual peaks reach 1800 m). Therefore since  $\sim 75\%$  of the AOD occurs above the altitude of the mountain ridge for the measurement period, this may explain the high correlation between these sites separated by the mountains (Figure 4) since the mountain ridge may not act as an effective barrier to advection for most of the aerosol layer.

[20] The daily average Angstrom exponent (440–870 nm) between the SMART and Jabal Hafeet sites was also highly correlated ( $r^2 = 0.90$ ), with the time period (11 August to 3 October 2004) average being 0.54 at Jabal Hafeet and 0.49 at SMART. The range in daily average  $\alpha$  differences (Jabal–SMART) from +0.18 to  $-0.11$ , with an average difference of 0.05, suggests that there was on average a slightly higher fraction of the total optical depth in the fine mode particle size range above the altitude of the mountain as compared to the layer between the ground and 800 m above ground level (consistent with the aircraft observations of Reid et al. (submitted manuscript, 2007a)). A similarly high correlation between column water vapor ( $r^2 = 0.89$ ) at these two sites also occurred. The average column water vapor ratio (Jabal Hafeet/SMART) was 0.68 with daily averages ranging from 0.55 to 0.79. Therefore, on average during 11 August to 3 October 2004, a higher percentage of the total column water vapor (32%) occurred in lowest

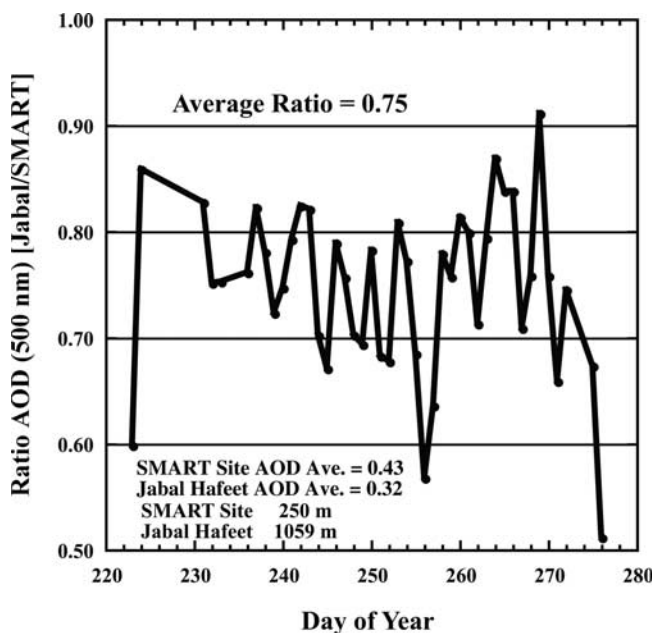


**Figure 5.** Ratio of aerosol optical depth (AOD) at the Jabal Hafeet site to the AOD at the SMART site, showing that over this time period (11 August to 3 October 2004), 25% of the aerosol in the total column was in the lowest 800 m above ground level.



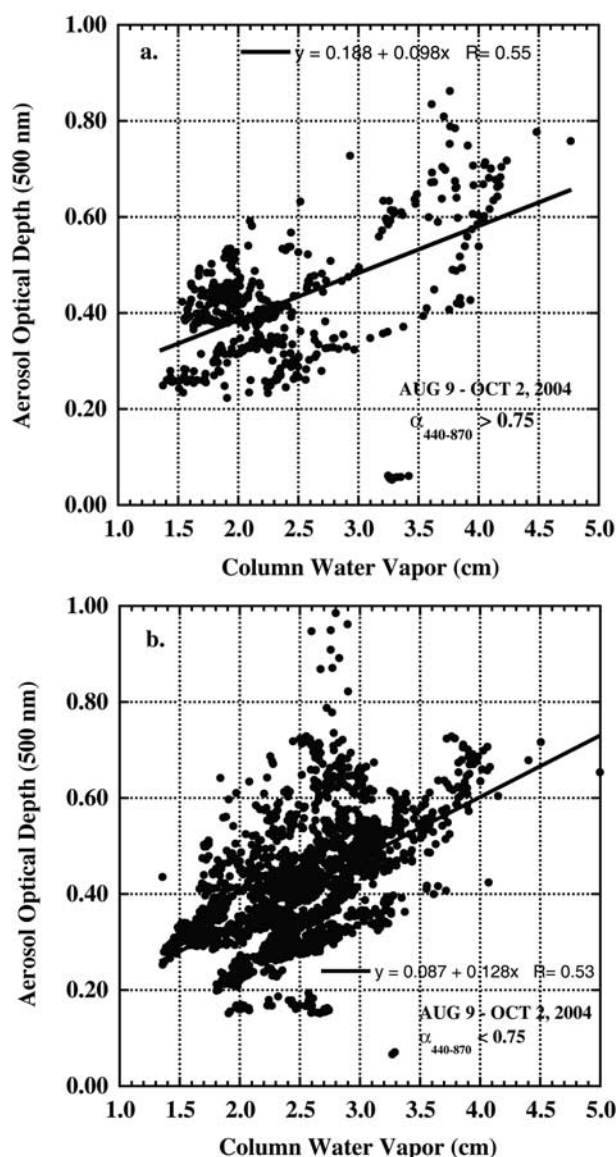


**Figure 6.** Relationship between aerosol optical depth and total column precipitable water at Hamim for instantaneous observations made where (a)  $\alpha_{440-870} > 0.75$  and (b)  $\alpha_{440-870} < 0.75$ .

800-m layer than did the percentage of the total column aerosol optical depth (25%).

### 3.1.5. Regional Comparison: Relationship Between AOD and Columnar Water Vapor

[21] In order to accurately assess the full atmospheric influence on regional radiative forcing it is important to understand the possible relationship between AOD and total column water vapor (CWV). The relationship between AOD (500 nm) and total column water vapor at Hamim is shown in Figure 6. Comparisons are made separately for coarse mode dominated cases ( $\alpha < 0.75$ ) and for fine mode dominated cases ( $\alpha > 0.75$ ). For both fine mode- and coarse mode dominated cases, there is an obvious trend of increasing AOD as CWV increases, characterized by similar degrees of correlation ( $r = 0.53$  for  $\alpha < 0.75$ ;  $r = 0.55$  for  $\alpha > 0.75$ ). The relationship of increasing AOD as CWV

increases seems independent of particle type (desert dust dominated or fine mode pollution). Additionally, the RH at this inland desert site was very low: the August to September average during daylight hours was  $\sim 36\%$  in 2004, resulting in insignificant humidification growth. Therefore it seems more likely that major aerosol sources are associated with atmospheric flow over the Arabian Gulf (principal regional source of atmospheric moisture) or that perhaps circulation convergence results in air that has both higher AOD and CWV. Similar correlation between AOD(500) and CWV was found for the Gulf island site of Sir Bu Nuair, although the correlation was higher for the fine mode dominated cases ( $r = 0.65$  for  $\alpha > 0.75$ ) than for the desert dust dominated cases ( $r = 0.47$  for  $\alpha < 0.75$ ). This suggests that aerosol hygroscopic growth may have a somewhat stronger influence for fine mode dominated events over the warm and humid Arabian Gulf. *Smirnov et al.* [2002b] similarly found increasing AOD(500) as CWV increased over Bahrain (a large island in the Arabian Gulf  $\sim 380$  km WNW of Sir Bu Nuair) in 1998–1999 for measurements made over the entire annual cycle. However, for fine mode cases they found a significantly higher correlation ( $r = 0.82$ ) while for coarse mode cases the correlation ( $r = 0.45$ ) was similar to what was observed in the UAE in summer.

### 3.1.6. Retrieval of Fine Mode Fraction From Spectral AOD

[22] Another sub goal of the UAE<sup>2</sup> mission was to study the fidelity of “fine mode fraction” algorithms. Based on the assumption that aerosol size distributions are bimodal, *O'Neill et al.* [2001, 2003] have developed a spectral deconvolution algorithm (SDA) that utilizes spectral AOD data to infer the component fine and coarse mode optical depths from the total extinction aerosol optical depth. The algorithm also fundamentally depends on the assumption that the coarse mode Angstrom exponent and its derivative are close to zero. The Angstrom exponent  $\alpha$  and the spectral variation of  $\alpha$  (as parameterized by  $\alpha' = d\alpha/d\ln\lambda$ ) are the measurement inputs to the SDA. These continuous-function derivatives (usually computed at a reference wavelength of 500 nm) are derived from a second-order fit of  $\ln \tau_a$  versus  $\ln \lambda$  [Eck et al., 1999]. The spectral AODs employed as input to the SDA were limited to the CIMEL wavelengths ranging from 380 to 1020 nm.

[23] Computed fine mode fractions from the SDA algorithm for the Sir Bu Nuair and Hamim sites for 1 August to 3 October 2004 are shown in Figure 7. These sites were chosen for comparison since their temperatures and relative humidity differ significantly, with lower temperatures and much higher RH over the Sir Bu Nuair Gulf island site and higher temperatures and much lower RH over the Hamim site, located in the desert  $\sim 125$  km inland from the Gulf. The fine mode fraction of the total aerosol optical depth at 500 nm is plotted as a function of  $\alpha_{440-870}$ . It is noted that as  $\alpha$  increases the fine mode fraction at Sir Bu Nuair is increasingly higher than at Hamim, although only slightly so. The much higher RH at Sir Bu Nuair is expected to result in significant hygroscopic growth of the fine mode particles since there is a sulfate component to this mode (Ross et al., submitted manuscript, 2007). Retrievals of the size distributions from the AERONET data using the *Dubovik and King* [2000] algorithm enhanced for spheroid particle scattering [Dubovik et al., 2006] from these same

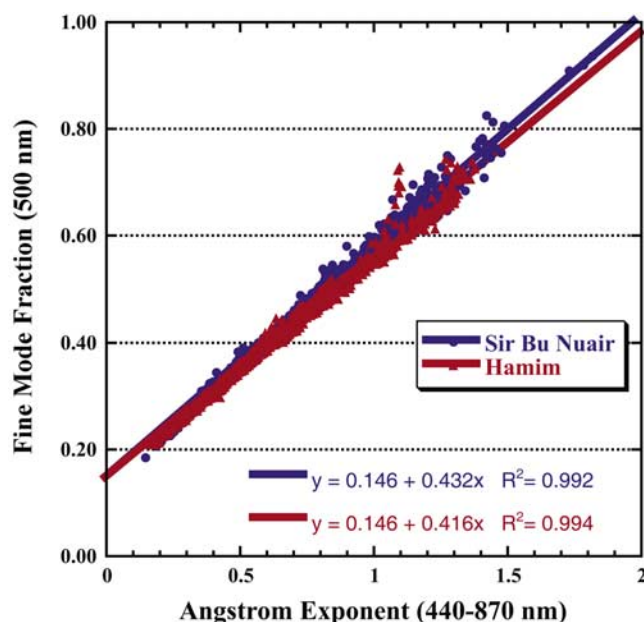


**Figure 7.** Fine mode fraction, computed from the O'Neill algorithm, versus measured Angstrom exponent ( $\alpha_{440-870}$ ) at Hamim and Sir Bu Nuair for 1 August to 2 October 2004. Data were screened to remove observations with missing or bad temperature measurements since at 1020 nm the detector is temperature sensitive, affecting the 1020-nm  $\tau_a$ .

sites do show somewhat larger fine mode particle radius values at Sir Bu Nuair than at Hamim (see section 3.2). Larger fine mode particles at Sir Bu Nuair than at Hamim is consistent with the larger computed fine mode fractions at Sir Bu Nuair for the same value of  $\alpha$ , especially for  $\alpha > 0.75$  when fine mode AOD begins to dominate the total AOD. However, differences in the magnitude of absorption between these 2 sites may also contribute to differences in the fine mode fraction as computed by the O'Neill algorithm. Mie calculations show that greater fine mode absorption results in lower values of both  $\alpha$  and  $\alpha'$  for a fine mode-only aerosol case [Eck *et al.*, 2001], as the wavelength dependence of scattering optical depth is greater than for absorption optical depth. Thus greater absorption at Hamim (see section 3.2) may also contribute somewhat to computation of smaller fine mode fraction values than for Sir Bu Nuair from the O'Neill algorithm. Nonetheless, even given some differences in particle size and absorption between these 2 sites, there is only a relatively small difference in computed fine mode fraction for a given  $\alpha$  (average fine fraction difference of  $\sim 0.02$  at  $\alpha = 1.2$  and 0.00 at  $\alpha = 0.3$ ), and the relationship of  $\alpha$  versus fine mode fraction shown in Figure 7 is very informative in the interpretation of the Angstrom exponent in this region. For example, from Table 2 we see that given the measured  $\sim 2$ -month mean of  $\alpha$  at Sir Bu Nuair of 0.77, the O'Neill algorithm computes a mean fine mode fraction of  $\sim 48\%$ , while for Hamim with a mean  $\alpha$  of  $\sim 0.57$  the O'Neill computed mean fine mode fraction is  $\sim 38\%$ . It is emphasized however that the relationship between fine mode fraction and  $\alpha$  shown in Figure 7 is representative only for the Arabian Gulf region, since large differences in  $\alpha$  may be caused by differences in fine mode

particle size that result from coagulation [Reid *et al.*, 1999] and other particle growth processes. For example, Eck *et al.* [2003] found that  $\alpha_{440-870}$  ranged from  $\sim 1.1$  to 2.0 for biomass burning smoke (fine mode fraction  $> 0.95$ ) with the lower  $\alpha$  values from cases of aged smoke with large size accumulation mode particles.

[24] We note that the linear relationship between fine mode fraction and Angstrom exponent is predicted by the bimodal equation [O'Neill *et al.*, 2003]:

$$\eta = \frac{\alpha - \alpha_c}{\alpha_f - \alpha_c} = \left( \frac{1}{\alpha_f - \alpha_c} \right) \alpha + \left( \frac{-\alpha_c}{\alpha_f - \alpha_c} \right) \quad (1)$$

where  $\alpha_f$  and  $\alpha_c$ , the Angstrom exponents of the fine and coarse mode, can be considered as (intensive variable) constants for a given fine and coarse mode distribution while  $\alpha$  is an extensive variable which varies with the coarse and fine mode loading. Equation (1) re-affirms and formalizes the qualitative explanation given above; an environment where fine mode particles are typically larger (i.e., such as Sir Bu Nuair) will be characterized by smaller values of  $\alpha_f$  and thus larger slope values and slightly smaller intercept values (with  $\alpha_c \sim -0.15$ , as per O'Neill *et al.* [2003]). This is precisely what the regressions of Figure 7 show. It should be noted that the Angstrom exponent employed in Figure 7 ( $\alpha_{440-870}$ ) should be  $\alpha(500 \text{ nm})$  to be coherent with equation (1). However, one can show that  $\alpha_{440-870}$  can be expressed as an approximate MacLaurin-type series in  $\alpha$  and  $\alpha'$  at 500 nm [O'Neill *et al.*, 2002]. Since  $\eta(500 \text{ nm})$  can also be expressed in terms of  $\alpha$  and  $\alpha'$  ( $\alpha_f$  in equation (1) is a weak function of  $\alpha$  and  $\alpha'$ ) it follows that  $\eta(500 \text{ nm})$  versus  $\alpha(400-870)$  actually produces a scattergram with dramatically less dispersion than  $\eta(500 \text{ nm})$  versus  $\alpha(500 \text{ nm})$ . This means that the slope of the scattergram will actually be somewhat less sensitive to the fine mode type but that only robustly systematic differences will be displayed.

### 3.2. AERONET Retrievals of Size Distributions and Single Scattering Albedo

#### 3.2.1. Comparison of Version 1 and Version 2 Retrievals

[25] The UAE<sup>2</sup> mission afforded one of the first opportunities to evaluate the AERONET version 2 almucantar retrievals. First, we consider dust-dominated air masses. Comparisons of retrievals between versions 1 and 2 for individual almucantar scans over desert (Hamim) and a dark water Arabian Gulf island site (Sir Bu Nuair) are given in Figure 8 with AOD(440) ranging from 0.44 to 0.92 for all cases shown. All version 1 retrievals in Figure 8 were made with the spheroid particle shape model, since the version 2 retrievals were dominated by spheroid-shaped particles (100% spheroids for both dust cases and 84% and 89% spheroids for the fine mode cases). Most cases shown are an average of 2–4 retrievals within a single morning or afternoon, while for some it is a single retrieval. The examples given in Figures 8a and 8b are desert dust dominated with low Angstrom exponent ( $\alpha_{440-870}$ ),  $\sim 0.15$  to 0.32. The single scattering albedo ( $\omega_0$ ) retrieved using version 1 for the dust aerosol in these cases showed relatively weak wavelength dependence and significant differences between the two sites, especially at 440 nm



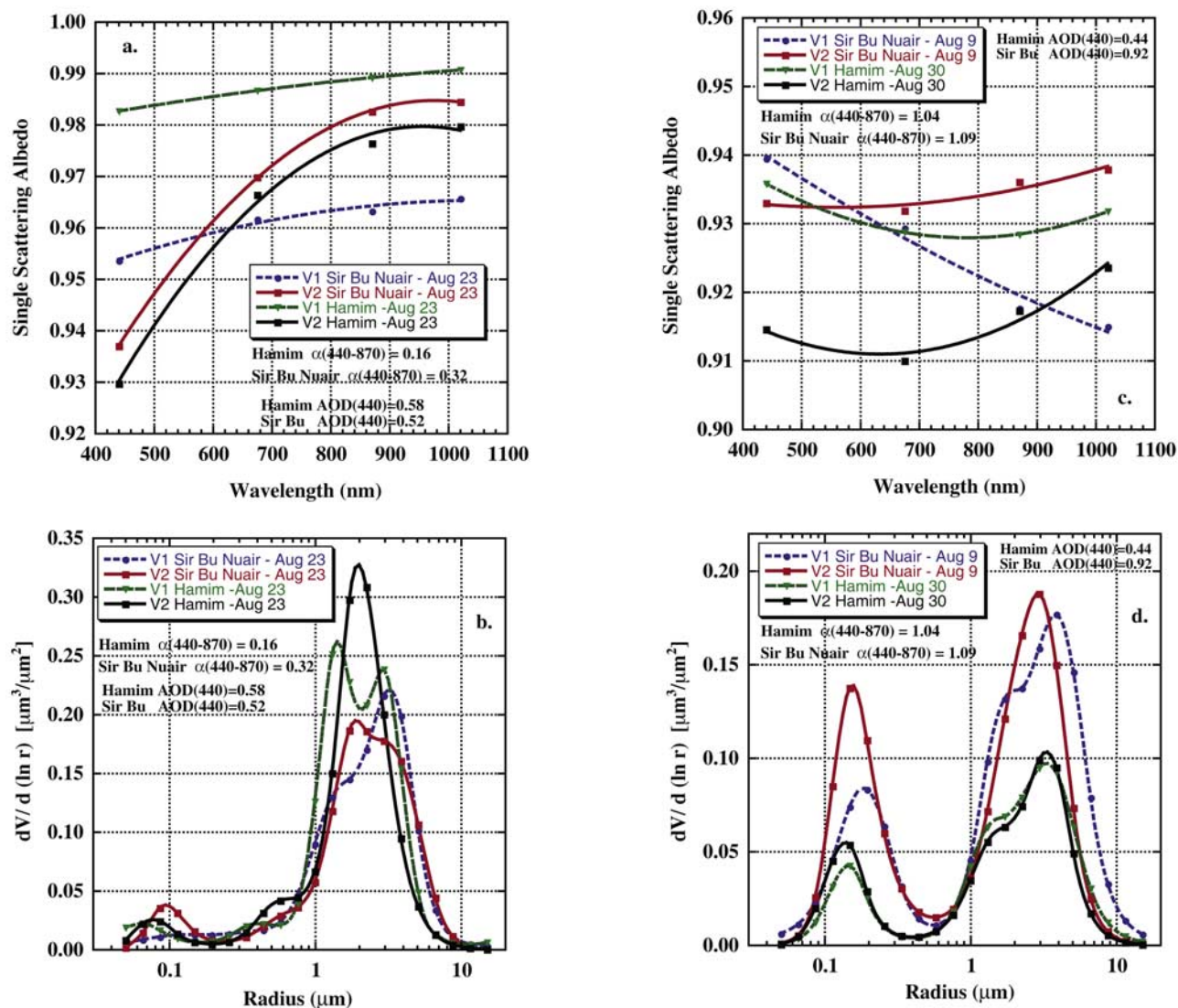


**Figure 8.** Comparison of version 1 versus version 2 AERONET almucantar retrievals of single scattering albedo and aerosol size distributions for (a and b) desert dust cases and for (c and d) fine mode pollution dominated cases.

where the discrepancy is  $\sim 0.03$ . For version 2, the differences in spectral  $\omega_0$  between sites were relatively small (less than 0.01 at all wavelengths) and the decrease at 440 nm relatively large. The decrease in  $\omega_0$  at short wavelength visible ( $<500$  nm) and ultraviolet wavelengths is typical of desert dust absorption for aerosol with an iron mineral component [Sokolik and Toon, 1999]. Most desert dust in this region is not likely to be hygroscopic [Li-Jones et al., 1998; Carrico et al., 2003]; therefore it would be expected that the absorption properties of the dust would be similar whether measured over the humid Arabian Gulf or over the very dry inland desert. The differences in the version 1  $\omega_0$  retrievals over the two sites were likely due to differences in surface reflectance that were not accounted for accurately.

[26] Comparison of the version 1 and 2 size distribution retrievals for these same desert dust cases are shown in Figure 8b. For the Hamim site the version 1 retrieved size distribution shows a bimodal coarse mode while for version 2 the coarse mode is unimodal. This bimodal nature is fairly

common in all previous version 1 retrievals of dust atmospheres [Reid et al., 2003]. However, it is also noted that there is less sensitivity to the size of coarse mode particles, as compared to fine mode size, in the AERONET retrieval since particles that are  $>1$  micron in radius all exhibit relatively little spectral variation in aerosol optical depth from 440 to 1020 nm, while changes in fine mode size affect both the linear (Angstrom) fit of  $\ln \tau_a$  versus  $\ln \lambda$  and the curvature or second-order polynomial fit. Therefore determination of particle size for the coarse mode depends almost solely on the angular sky radiance distribution, while for fine mode-size particles there is significant additional information in the spectral AOD in addition to the sky radiance distribution.

[27] In comparison, Figures 8c and 8d present version 1 and 2 retrievals for almucantar scans where a prominent fine mode was also present. For these scans the Angstrom exponent exceeded unity, 1.04 at Hamim and 1.09 at Sir Bu Nuair. The version 2 single scattering albedo retrievals



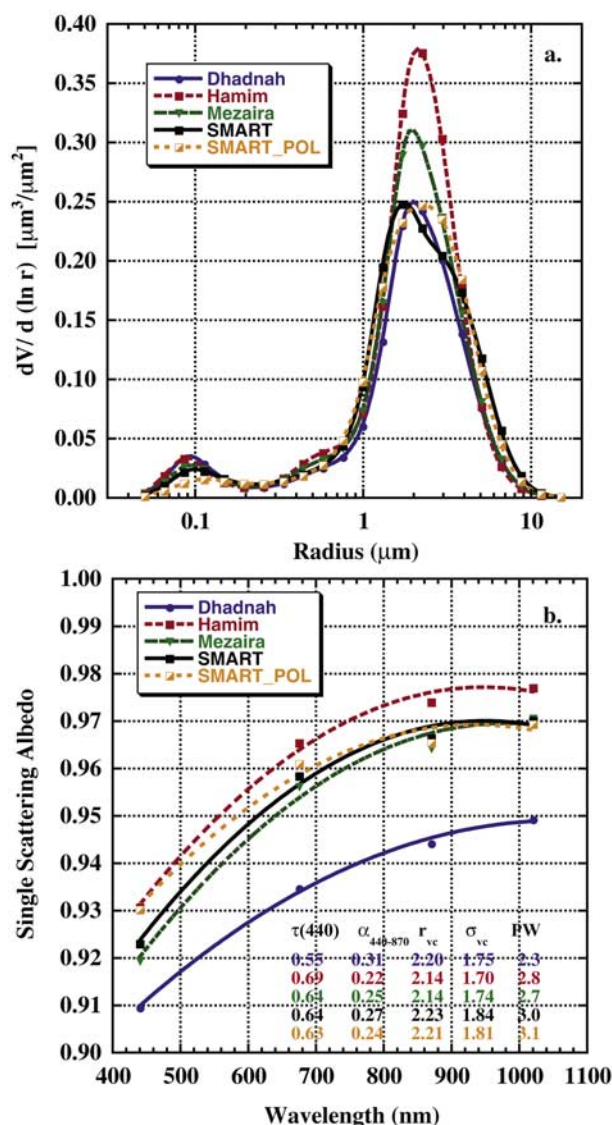


**Figure 9.** Comparison of AERONET retrievals of size distributions and single scattering albedo made at four different sites during a desert dust event on 22 September 2004.

for these two sites differ more from each other than the version 1 retrievals. These differences may reflect physical differences in aerosol absorption that result from the extreme contrast in relative humidity (RH) between the sites, in conjunction with the presence of hygroscopic fine mode particles (Ross et al., submitted manuscript, 2007). The higher version 2  $\omega_0$  at Sir Bu Nuair would be expected on the basis of the high RH (frequently above 70%) compared to the very dry desert air over Hamim. Comparison of the fine mode size distributions of these cases shows that for both sites there is a shift to somewhat smaller size particles in version 2 versus version 1 (especially for the Sir Bu Nuair case), while the volume median radius remained similar for the coarse mode.

[28] For these prominent fine mode cases, the new retrieval also resulted in changes in index of refraction. For the Sir Bu Nuair case, the retrieved real refractive index

decreased from 1.44 in version 1 to 1.37 in version 2, while for the Hamim case the real refractive index decreased from 1.52 in version 1 to 1.45 in version 2. In order to maintain retrieval optical depth, this shift to smaller sizes and indices of refraction must also coincide with a comparable increase in amplitude of the particle size distribution. Two month averages of version 2 retrievals of  $\omega_0$  and size distributions for the entire range of measured Angstrom exponents for these same two sites will be discussed later in section 3.2.3.

[29] From this analysis it is clear that significant differences do exist between the older and newer retrievals. These differences for the most part appear to be traced back to improved surface albedo parameterizations. Indeed, the new version 2 retrievals of dust aerosol single scattering albedo with much lower values in the blue are much closer to what we would expect [e.g., Sokolik and Toon, 1999; Bergstrom et al., 2002]. For the remainder of this manuscript, all subsequent AERONET inversion results presented are version 2 results of single scattering albedo and size distributions.

### 3.2.2. In-Depth Analyses of Retrievals for Coarse- and Fine Mode Dominated Events

#### 3.2.2.1. Coarse Mode Dominated Event of 22 September 2004

[30] On 22 September 2004 the AOD at most sites in the UAE was relatively high and the Angstrom exponent relatively low, thus indicating the dominance of coarse mode size particles. During this event regional winds were low, and it appears that dust generated in the UAE stagnated for several days, before being ventilated on 23 September. Consequently, AODs were regionally high and well spread over the region. For this event we compare AERONET almucantar retrievals for four sites spanning the UAE on this date: Dhadnah, Hamim, Mezaira, and SMART in Figure 9. The 440-nm AOD for these sites during the times of the retrievals ranged from 0.55 to 0.69 and the 440- to 870-nm Angstrom exponent ranged from 0.22 to 0.31. These  $\alpha$  values correspond to fine mode fractions of the total optical depth of only  $\sim 0.24$  to  $\sim 0.29$ , as estimated from the O'Neill algorithm (Figure 7). Seven-day back trajectories from the HYSPLIT model (see <http://www.arl.noaa.gov/ready/hysplit4.html>) for Hamim (Figure 10a) for the retrieval time on 22 September shows midboundary layer flow (final altitude 1500 m above ground level at Hamim) originating in Afghanistan and Iran and near surface trajectory coming from the south over the Indian Ocean, then over Oman and Saudi Arabia. The back trajectory for Dhadnah (Figure 10b) shows that the near surface trajectory is mainly over ocean except 6–7 days prior over coastal Somalia, while the trajectories ending at 1500 and 3000 m originate mainly from Iran, southern Pakistan and Turkmenistan.

[31] The volume size distributions for the four sites on 22 September are shown in Figure 9a. The coarse mode dominates and the particle size distributions are similar at all four sites, with the computed volume coarse mode median radius ranging from 2.14 to 2.23  $\mu\text{m}$ . The geometric standard deviation (width) of the size distributions also showed little variance among the sites, ranging from 1.70 to 1.84. For long-distance transported Saharan coarse mode dust in Puerto Rico, Reid et al. [2003] found a very large range in volume median radius of  $\sim 1.25$  to 4.5  $\mu\text{m}$

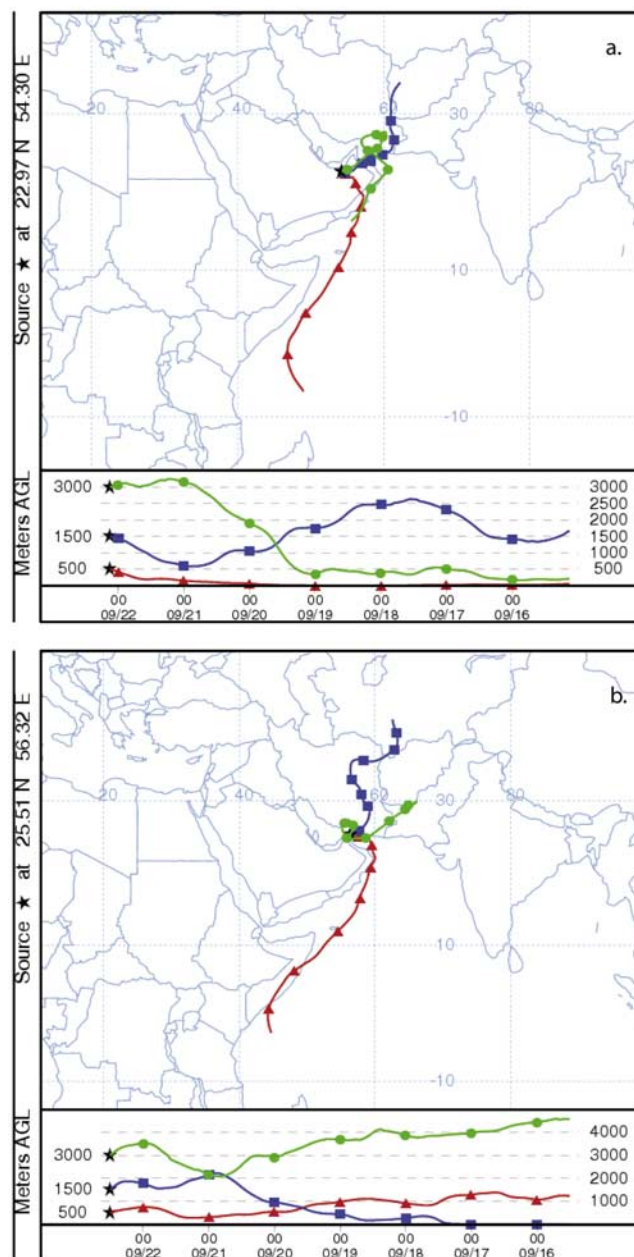


**Figure 10.** Seven-day back trajectories computed from the HYSPLIT model for 22 September 2004 (same date and times as data shown in Figure 9) for (a) the Hamim site and for (b) the Dhadnah site.

from a variety of in situ measurement techniques. They attributed these differences to various systematic biases for the different techniques. For in situ measurements made at the MAARCO site during UAE<sup>2</sup>, Reid et al. (submitted manuscript, 2007b) found volume median radius ranging from 1.63 to 2.28  $\mu\text{m}$  (geometric standard deviation ranging from 1.78 to 2.16), with size differing for the various dust source regions (northern UAE/Iran, Iraq, southern Oman/Yemen, local UAE).

[32] The retrievals of single scattering albedo for these same retrievals are shown in Figure 9b. The spectral  $\omega_0$  are

similar at all four sites, especially for Hamim, Mezaira, and SMART which are within  $\sim 0.01$  of each other for all 4 wavelengths. Although the  $\omega_0$  at Dhadnah are  $\sim 0.01$  to 0.02 lower than at the SMART site, these differences are still within the range of uncertainty of the retrievals ( $\sim 0.03$ ). The lower  $\omega_0$  at Dhadnah may be due to real differences in the aerosol absorption (see different near surface trajectories in Figure 10) or possibly due to greater uncertainty in surface albedo. Since Dhadnah is near the coast ( $\sim 2$  km), the specification of the correct surface albedo and BRDF is much more difficult and complex since the surfaces near this site (desert, mountains, and ocean) have very different reflectance magnitudes as a function of solar zenith angle and also extremely different BRDF shapes (forward scatter glint from ocean versus backscatter maximum over land). We combine the mixture of land and ocean surface BRDF values using weighting by the land-ocean percentage and creating a mixture BRDF that does not account for land surface slope effects such as from hills or mountains.

[33] At the SMART site, two CIMEL Sun-sky radiometers were operated side by side. The retrievals of  $\omega_0$  for these 2 CIMELs at SMART agree to within less than 0.01 for all four wavelengths, suggesting consistent instrument performance and calibration accuracy. The size distribution retrievals for the two SMART site instruments show some minor differences in both fine and coarse modes; however, the computed coarse mode median volume radius was very similar for both, 2.21 and 2.23  $\mu\text{m}$ , with similar coarse mode geometric standard deviations also, 1.81 and 1.84.

### 3.2.2.2. Fine Mode Dominated Event of 1 September 2004

[34] On 1 September 2004 the Angstrom exponents measured at all AERONET sites in the UAE were relatively high and the AOD mostly above the 2-month mean (Figure 2, day 245). We present the results of AERONET almucantar retrievals from 4 sites on 1 September in Figure 11, with one site (Hamim) on 31 August since there were no good retrievals with high  $\alpha$  on 1 September at that site. The 440-nm AOD for these sites during the times of the retrievals ranged from 0.50 to 0.82 and the 440- to 870-nm Angstrom exponent ranged from 1.02 to 1.33. These  $\alpha$  values correspond to fine mode fractions of the total optical depth of  $\sim 0.57$  to  $\sim 0.70$  (relatively high for the UAE), as estimated from the O'Neill algorithm (Figure 7). However, there is still  $\sim 30$  to 40% coarse mode fraction for these data and therefore the coarse mode still has significant influence on optical properties even during this pollution event.

[35] The 30 August to 1 September pollution event brought the highest levels of fine mode particles to the UAE during the entire study. Twenty-four hour particulate matter with diameter  $< 2.5 \mu\text{m}$  ( $\text{PM}_{2.5}$ ) concentrations measured at the MAARCO site topped 100  $\mu\text{g m}^{-3}$  (Ross et al., submitted manuscript, 2007). The event was a result of a flow reversal, where previously winds were strong southwesterly. Then starting approximately on 29 August, winds reversed to the more typical northwesterly monsoonal flow (Reid et al., submitted manuscript, 2007a). A consequence was that the air mass reaching the UAE during the event period spent many days over the Arabian Gulf as demonstrated by the HYSPLIT model seven-day back trajectory analysis for Sir Bu Nuair (Figure 12a). For the retrieval time on 1 September the trajectory analysis shows boundary



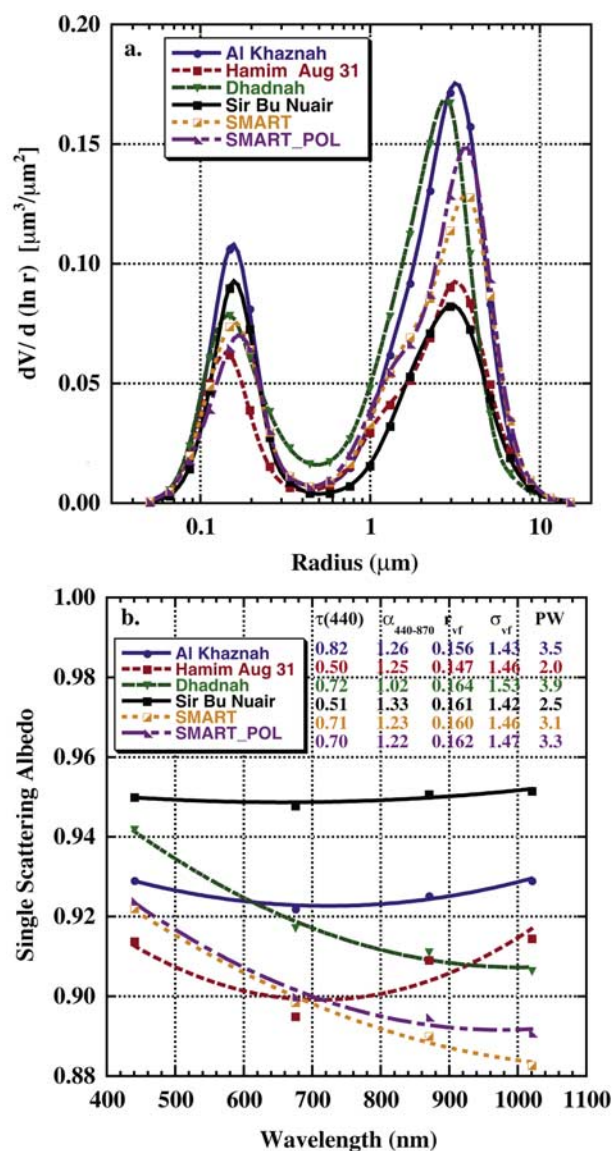


**Figure 11.** Comparison of AERONET retrievals of size distributions and single scattering albedo made at five different sites during a pollution event on 1 September 2004 (31 August 2004 for Hamim).

layer flow at all levels for the prior two days to be nearly parallel to and over the Arabian Gulf and adjacent coastal lands. Most petroleum processing sites are located on islands, platforms and coastal regions and produce significant amounts of sulfate-based particles throughout the Arabian Gulf (Ross et al., submitted manuscript, 2007). Back trajectories for the SMART, Al Khaznah, and Hamim sites on 1 September (31 August for Hamim) also show that air parcels transited over the Arabian Gulf for the prior two to four days on at least one of the three levels. The back trajectory for Dhadnah (Figure 12b) is quite different however, with only the upper-level trajectory (altitude at 3000 m on 1 September) over the Arabian Gulf for only 1 day and the surface trajectory over the Gulf of Oman for 2 days, and with the flow at all levels directly from the north over Iran for the majority of the seven-day back trajectory.

The lower Angstrom exponent at Dhadnah (1.02) compared to a range of 1.22 to 1.33 at the other 4 sites is consistent with the longer transport time over land for the Dhadnah air parcels.

[36] The retrievals of  $\omega_0$  for the 2 CIMEL Sun-sky radiometers at SMART agree to within  $\sim 0.01$  or less for all four wavelengths, again suggesting consistent instrument performance and calibration accuracy. The size distribution retrievals for the two SMART site instruments show some minor differences in both fine and coarse modes; however, the computed fine mode volume radius was very similar for both, 0.160 and 0.162  $\mu\text{m}$ , with nearly the same fine mode

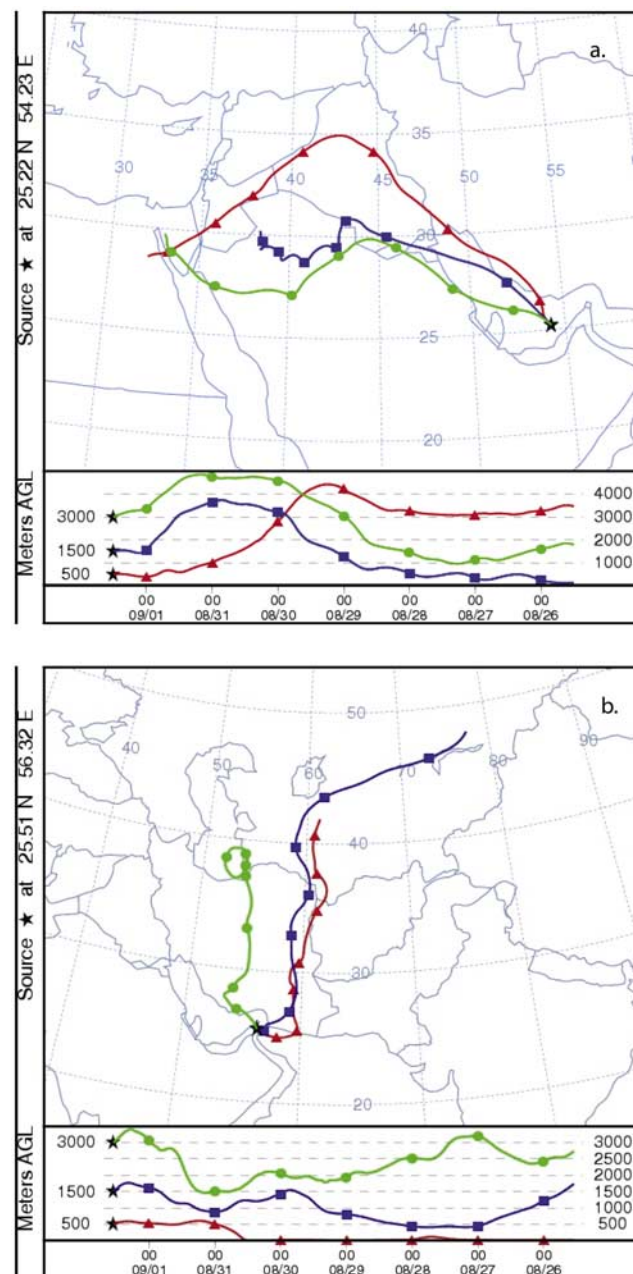


**Figure 12.** Seven-day back trajectories computed from the HYSPLIT model for 1 September 2004 (same date and times as data shown in Figure 11) for (a) the Sir Bu Nuair site and for (b) the Dhadnah site.



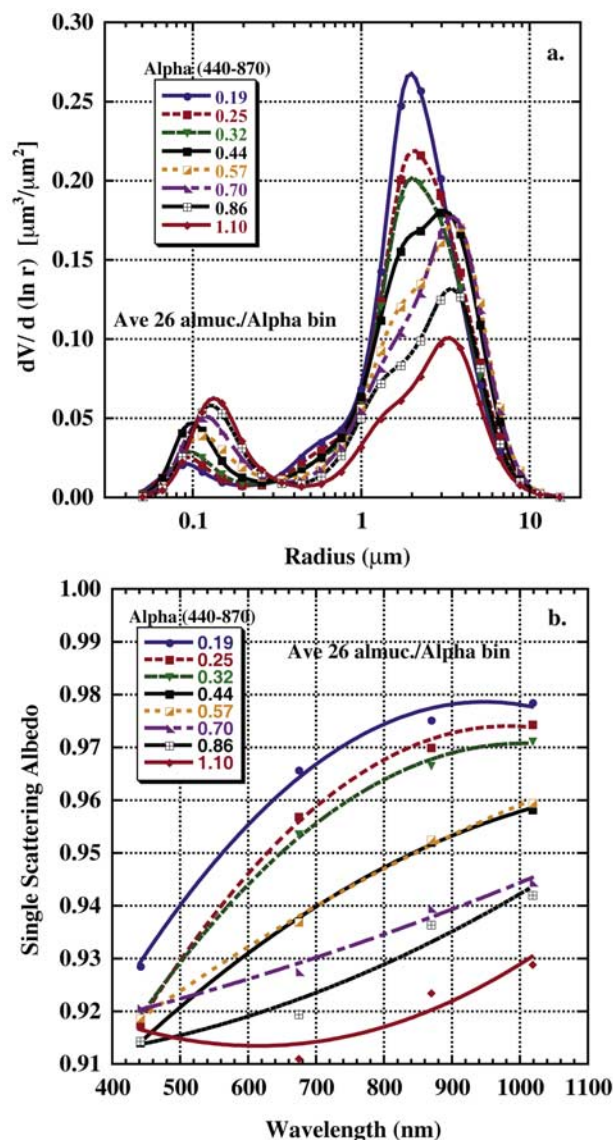


**Figure 13.** Average size distributions and single scattering albedos as a function of Angstrom exponent ( $\alpha_{440-870}$ ) for Hamim for 1 August to 4 October 2004 for almucantar scans with  $\tau_{a440} > 0.4$ . There are 26 almucantar scan retrievals averaged for each Angstrom exponent bin.

geometric standard deviation, 1.46 and 1.47. These differences are insignificant, and attest to the repeatability of retrievals made with co-located instruments.

[37] Comparison of  $\omega_0$  for these five sites (Figure 11b) shows that the three westernmost sites display no significant wavelength dependence while the easternmost sites (Dhadnah and SMART) are characterized by decreasing  $\omega_0$  as wavelength increases. The Arabian Gulf island site (Sir Bu Nuair) has the weakest absorption, which would be consistent with a large fine mode radius ( $0.161 \mu\text{m}$ ) resulting from hygroscopic growth induced by high humidity. The sites with the lowest  $\omega_0$ , especially at 440 and 675 nm, are the inland desert sites of Hamim and SMART. Hamim has relatively small particle radius ( $0.147 \mu\text{m}$ ), while the SMART site has large radius particles ( $\sim 0.161 \mu\text{m}$ ). Higher

column water vapor at the SMART site (3.2 cm) than at Hamim (2.0 cm) suggest different transport pathways. The comparison in Figure 11 suggests relatively large variability in absorption among the five sites on this date ( $\omega_0$  range of  $\sim 0.04$  at 440 nm and  $\sim 0.07$  at 1020 nm) possibly due to differences in chemical composition of both fine and coarse modes, but also possibly due in part to uncertainty in surface albedo that differs significantly between sites (brighter sandy desert versus darker water surrounding the Arabian Gulf island). However, the uncertainty in surface albedo may be less important since the  $\omega_0$  spectral dependencies for dust cases were consistent (Figure 9b).

### 3.2.3. Size Distributions and Single Scattering Albedo As a Function of Angstrom Exponent

[38] In this section we analyze the average characteristics of the AERONET retrievals of aerosol size distribution and single scattering albedo as they vary over the observed range of Angstrom exponent. Two sites in contrasting environments are analyzed in detail: Hamim located inland in a sandy desert region with low RH and very high surface temperature, and Sir Bu Nuair located on an island in the Arabian Gulf, with very high RH and lower (but still high) surface temperature. All high-quality (AERONET version 2, level 2.0) almucantar retrievals made over the 2-month period of 1 August through 4 October 2004 were grouped into eight bins of Angstrom exponent (Figures 13 and 14). For the Hamim site (Figure 13), the analysis includes 26 almucantar retrievals averaged for each Angstrom exponent bin with bin average  $\alpha$  ranging from 0.19 to 1.10. For the Sir Bu Nuair site (Figure 14), there are 15 almucantar retrievals averaged for each Angstrom exponent bin with average  $\alpha$  ranging from 0.32 to 1.25.

[39] The fine mode size distribution retrievals at both Hamim and Sir Bu Nuair show trends of increasing radius as Angstrom exponent increases (Figures 13a and 14a). These trends suggest the possibility that fine mode dust particles may be smaller in size than fine mode pollution particles. Few publications have compared or evaluated the size distribution of fine mode dust particles, but a study has shown that fine mode dust particles are generated in dust events by sandblasting processes [Gomes *et al.*, 1990]. However, Reid *et al.* (submitted manuscript, 2007a) did not detect a strong submicron dust mode with surface in situ measurements at MAARCO during the UAE<sup>2</sup> campaign, except for very small fine dust (radius  $\sim 0.125 \mu\text{m}$ ) originating from Iraq. Fine mode optical depth at 500 nm (as estimated from the O'Neill algorithm) for the  $\alpha$  bins shown in Figure 13 (and Figure 14) varied from  $\sim 0.12$  at  $\alpha = 0.20$  to  $\sim 0.26$  at  $\alpha = 1.12$  at Hamim (from  $\tau_{f500} \sim 0.16$  at  $\alpha = 0.34$  to  $\tau_{f500} \sim 0.42$  at  $\alpha = 1.21$  at Sir Bu Nuair). The concentrations of fine mode particles in most cases were probably too low to result in significant growth by coagulation. Another possible factor in the fine mode size trend is that the small size fine mode particles retrieved for dust dominated cases may result from low sensitivity to the fine mode particles when the coarse mode dominates, and therefore these smaller particle sizes for low- $\alpha$  cases may be partly an artifact of the retrieval.

[40] For the largest Angstrom exponent bin averages for each site (1.10 at Hamim and 1.25 at Sir Bu Nuair), the peak value in the fine mode size distribution occurred at  $\sim 0.135 \mu\text{m}$  at Hamim and  $\sim 0.16 \mu\text{m}$  at Sir Bu Nuair. This

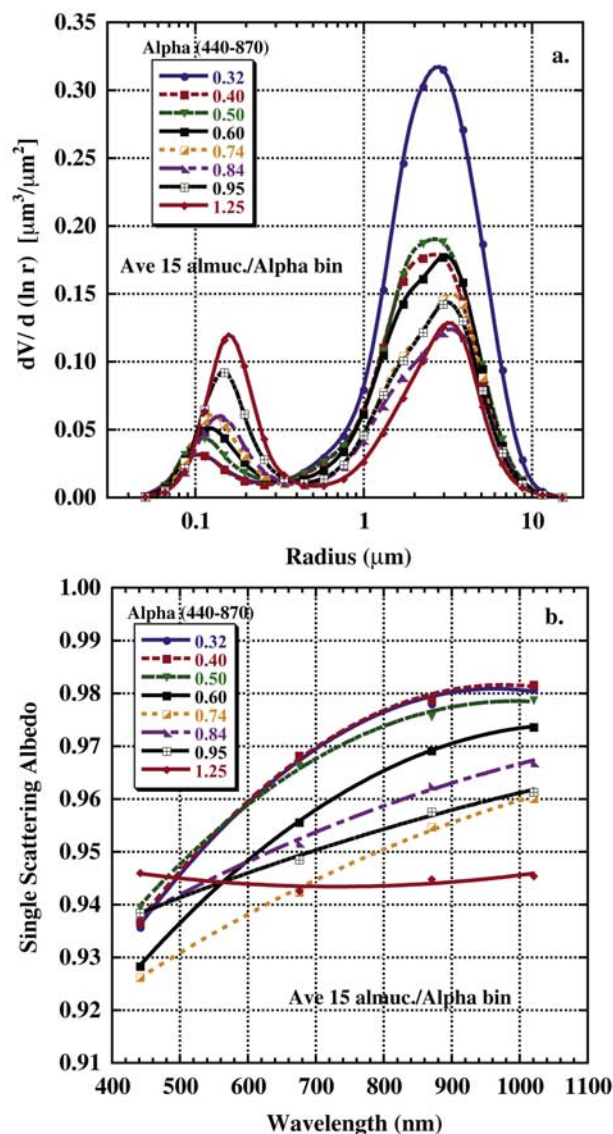


**Figure 14.** Average size distributions and single scattering albedos as a function of Angstrom exponent ( $\alpha_{440-870}$ ) for Sir Bu Nuair for 1 August to 4 October 2004 for almucantar scans with  $\tau_{a440} > 0.4$ . There are 15 almucantar scan retrievals averaged for each Angstrom exponent bin.

size difference may result from the much higher relative humidity over the Sir Bu Nuair site, which could foster greater hygroscopic growth.

[41] The average size distribution retrievals at Hamim suggest that the coarse mode is slightly bimodal at times (Figure 13a). This results from individual retrievals exhibiting a somewhat bimodal coarse mode, rather than averaging of individual unimodal coarse mode retrievals of two different sizes. However, we do not place much significance or confidence in whether the coarse mode is really bimodal, since the retrievals have less sensitivity to coarse mode particle size in this size range, as compared to fine mode particle size. One of the input data sets to the almucantar inversion, the spectral aerosol optical depth from 440 to 1020 nm, has minimal information on particle size for

particles  $\sim 1$  micron and larger. The Angstrom exponent for super micron coarse mode particles is nearly zero with small spectral variability [O'Neill *et al.*, 2001]. The mean volume median radius of the coarse mode at Hamim ranged from  $\sim 2.1$  to  $2.2 \mu\text{m}$  ( $\sim 2.2$  to  $2.5 \mu\text{m}$  at Sir Bu Nuair) with geometric standard deviation of 1.75 to 1.81 ( $\sim 1.80$  to  $1.82$  at Sir Bu Nuair) for retrievals made during dust dominated events ( $\alpha_{440-870} < 0.4$ ).

[42] The variation in aerosol single scattering albedo as a function of the Angstrom exponent is shown for both Hamim and Sir Bu Nuair in Figures 13b and 14b, respectively. Comparison of the spectral  $\omega_0$  at these sites for the lowest Angstrom exponent bins ( $\alpha$  ranging from 0.19 to 0.32, therefore strong dust domination) shows that the values agree with each other to within  $\sim 0.01$  to  $0.015$  at all wavelengths, well within the uncertainty of the retrievals of  $\sim 0.03$ . Relative spatial homogeneity in average dust absorption properties is to be expected over the UAE desert and the Arabian Gulf since the dust originates from the same or similar source regions and since most of the mineral dust aerosol is not hygroscopic [Li-Jones *et al.*, 1998; Carrico *et al.*, 2003], and therefore does not change properties as a function of relative humidity. The mean midvisible (550 nm) single scattering albedo determined from in situ measurements on aircraft flights in elevated dust layers near Korea and Japan was  $\sim 0.96$  [Anderson *et al.*, 2003], which is similar to the AERONET measured values in the UAE of  $\sim 0.94$ – $0.95$ , interpolated to 550 nm (Figures 13b and 14b).

[43] In contrast to spectral  $\omega_0$  for the low Angstrom exponent bins, there is a significant difference in the magnitude between Sir Bu Nuair and Hamim for the highest Angstrom bins ( $\alpha = 1.25$  and  $1.10$  respectively). In the visible wavelengths (440 and 670 nm) the difference is  $\sim 0.03$ , with higher values at Sir Bu Nuair of  $\sim 0.945$  at 440 nm versus  $\sim 0.915$  at Hamim. This is consistent with the larger values of fine mode peak radius at Sir Bu Nuair compared to Hamim (as discussed previously), being likely due to hygroscopic particle growth under high relative humidity conditions at Sir Bu Nuair. The location of a petroleum processing complex between Hamim and the Arabian Gulf coast and the location of several island and offshore platform petroleum extraction and processing facilities in the general vicinity of Sir Bu Nuair also presents the possibility that more or less black carbon is emitted in the aerosol mixtures near these two sites, thus contributing to the observed differences in absorption. The same type of analysis for the Mezaira site, located  $\sim 55$  km west–northwest of Hamim, shows the fine mode dominated  $\omega_0$  at  $\alpha = 1.10$  (average of 24 almucantars) to be similarly spectrally flat and within  $< 0.01$  of the values retrieved at Hamim. The average fine mode dominated  $\omega_0$  at  $\alpha = 1.22$  (average of 5 almucantars) at the Umm Al Quwain site located only  $\sim 1$  km inland from the Gulf also shows nearly spectrally neutral values within  $< 0.01$  of the retrievals at Sir Bu Nuair. These comparisons suggest that there is real regional variation in fine mode single scattering albedo with significantly less absorption occurring over the Gulf and coastal regions than over the desert. The relatively wavelength invariant  $\omega_0$  for the fine mode dominated cases in the UAE contrasts with fine mode spectral dependence retrieved at other AERONET sites in the world, owing to a



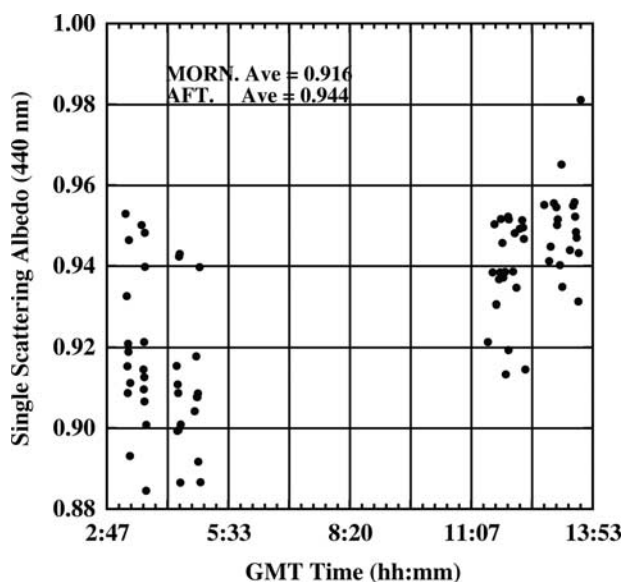


**Figure 15.** Morning versus afternoon AERONET retrievals of single scattering albedo (440 nm) at the MAARCO site, for the time interval 27 August through 30 September 2004. Retrievals are made for the same range of solar zenith angles,  $53^\circ$  to  $77^\circ$ , in the morning and the afternoon. Local time is UTC + 3, for comparison to Figure 3.

larger fraction of coarse mode particles present in the UAE. Therefore the persistence of coarse mode particles in this region, even during pollution events, results in the longer-wavelength AOD being dominated by super micron size dust particles, thus resulting in weaker absorption as wavelength increases. A comparison of the spectral  $\omega_o$  at several urban regions in the world dominated by fine mode aerosol [Eck *et al.*, 2005] shows that for locations with highly absorbing aerosol (Mexico City, Beijing and the Maldives) the slope as a function of wavelength is the shallowest for Beijing owing to the greater fraction of coarse mode particles at that site. Spectrally decreasing  $\omega_o$  with increasing wavelength for fine mode dominated aerosols (when the coarse mode is not significant) results from a relatively constant imaginary part of the refractive index that is typical of black carbon absorption [Bergstrom *et al.*, 2002; Eck *et al.*, 2003].

[44] The spectral  $\omega_o$  measured over Hamim, for all wavelengths except 440 nm, decreased significantly as the Angstrom exponent increased (Figure 13b). This results from mixtures of weakly absorbing coarse mode aerosols with relatively strongly absorbing fine mode aerosol. The total-column radiatively effective aerosol “mixtures” may result from different aerosol types being located in layers at different altitudes above the surface as was commonly observed during ACE-Asia [Schmid *et al.*, 2003; Redemann *et al.*, 2003], mixed fine and coarse mode aerosols present in the same layers, and also possibly from the coating of large dust particles with fine mode black carbon and other species. The aggregation of fine mode black carbon particles on the surface of coarse mode dust was commonly observed in scanning electron microscopy (SEM) images of aerosol samples obtained in South Korea during the ACE-Asia field experiment [Arimoto *et al.*, 2006]. Typically

$\sim 15\%$  to  $30\%$  of the surface of dust particles they sampled were coated by black carbon, thus most likely increasing absorption and therefore lowering the  $\omega_o$ . It is not known to what extent this process of dust particle aggregation with fine mode particles including black carbon occurred in the UAE environment. The 440-nm single scattering albedo at Hamim did not change much ( $\sim 0.01$ ) as a function of varying Angstrom exponent since the coarse mode dust is relatively strongly absorbing at this wavelength (owing to absorption by iron oxides) and similar in magnitude to the  $\omega_o$  of the fine mode pollution.

### 3.2.4. Diurnal Trends in Aerosol Absorption

[45] The diurnal variability of aerosol absorption was investigated by Remiszewska *et al.* [2007] using surface based in situ measurements at a coastal site (MAARCO) approximately 60 km northeast of Abu Dhabi. They found a large diurnal cycle in single scattering albedo with an average diurnal range of  $\sim 0.08$  at 450 nm, a minimum of  $\sim 0.88$  in early morning and nearly linearly increasing to a maximum of  $\sim 0.96$  near midnight, during the time period 27 August to 30 September 2004. This daily cycle in aerosol absorption is explained by Remiszewska *et al.* [2007] as being related to the cycle of the sea breeze circulation, which brings in cleaner air during the day while at night the relatively stagnant air allows more absorbing pollutants to accumulate.

[46] Figure 15 presents the column integrated  $\omega_o$  at 440 nm inferred from AERONET retrievals at MAARCO from 27 August to 30 September 2004 (same time period) for morning and afternoon time periods where the solar zenith angle range in both intervals is  $53^\circ$ – $77^\circ$  and  $\tau_{a440} > 0.40$ . At  $\sim 0400$  UTC (0800 LST) the AERONET retrieval average  $\omega_o$  at 440 nm is  $\sim 0.916$  while at  $\sim 1230$  UTC the column average is  $\sim 0.944$ , or  $\sim 0.03$  higher. At the surface, the in situ based measurements at the same times were  $\sim 0.88$  at 4 UTC and  $\sim 0.93$  at 1230 UTC [Remiszewska *et al.*, 2007], thus exhibiting a larger increase than the column integrated retrievals. This may be the result of greater absorption dynamics in the lower boundary layer and/or greater diurnal range in days with lower AOD since AERONET retrievals are analyzed only for conditions when  $AOD(440) > 0.4$  (since uncertainty is higher at low AOD). The AERONET direct Sun measurements of Angstrom exponent (440–870 nm) computed from extinction aerosol optical depth (coinciding with the almucantar retrievals) show no significant change between the morning and afternoon, with an average of 0.620 in the morning versus 0.605 in the afternoon. This contrasts with the in situ based Angstrom exponent (450–700 nm) computed from scattering coefficients which increased from  $\sim 0.85$  to  $\sim 1.0$  for the times of the AERONET retrievals [Remiszewska *et al.*, 2007]. Additionally, the minimum to maximum daytime diurnal cycle in  $\alpha_{440-870}$  from AERONET is  $\sim 0.08$  at MAARCO (see Figure 3) while for the same time interval (daylight hours) the in situ nephelometer measured 450- to 700-nm Angstrom exponent range was  $\sim 0.25$  or a factor of 3 greater [Remiszewska *et al.*, 2007]. This suggests that the diurnal dynamics in aerosol size distribution is dominated by changes in the lower boundary layer. The columnar aerosol optical depth from AERONET measurements (during the almucantar scans with  $\tau_{a440} > 0.4$ ) was higher in the morning, 0.59 at 440 nm versus 0.49 in the afternoon,



although this  $\sim 17\%$  drop in AOD still results in a high column aerosol loading in the afternoon.

[47] The same analysis was performed for other AERONET sites during the UAE<sup>2</sup> campaign to further investigate the diurnal variability of absorption. The Al Qlaa site which is also on the coast [ $\sim 200$  km west–southwest of Abu Dhabi, in a less industrialized area] showed essentially no difference in morning versus afternoon retrievals of  $\omega_0$  at 440 nm with averages of 0.940 in the morning versus 0.943 in the afternoon for a different time period, 23 June to 24 August 2004 (the instrument was removed on 25 August). There is somewhat greater uncertainty in AERONET retrievals of  $\omega_0$  at coastal sites owing to difficulty in accurately characterizing the BRDF of mixed land–ocean scenes and how this changes with solar azimuth; however, this uncertainty and possible bias may be similar for both the MAARCO and Al Qlaa sites. This suggests that differences between the MAARCO and Al Qlaa sites were real and thus the proximity of the urban plume from Abu Dhabi to the MAARCO site may have contributed to the significant diurnal variation in absorption at that site, which may not necessarily be representative of other coastal sites in the region. There was also no significant diurnal variation ( $<0.01$ ) in AERONET retrieved  $\omega_0$  at the inland desert site of Hamim or the Arabian Gulf island site of Sir Bu Nuair (for observations where  $\text{AOD}(440) > 0.4$ ) during the months of August through September 2004. Diurnal cycles in absorption would be less likely at these locations owing to the lack of significant influence of diurnal sea breeze and land breeze circulations.

#### 4. Summary and Conclusions

[48] The United Arab Emirates Unified Aerosol Experiment (UAE<sup>2</sup>) field campaign was conducted in the summer of 2004 (primarily August and September) in order to characterize aerosol properties in the region and to improve aerosol remote sensing over high reflectance surfaces. As a component of this experiment a mesoscale network of 14 AERONET Sun–sky radiometers was installed in the UAE and adjacent Arabian Gulf waters. The principal findings of the analyses of these measurements are given below.

[49] 1. The aerosol loading in the southern Arabian Gulf and UAE region in August to September 2004 was high with  $\tau_{a500}$  averaging from 0.40 to 0.53 over several sites. However, there was significant temporal variability, with daily average  $\tau_{a500}$  ranging from  $<0.2$  to  $>1.0$  and also in daily average  $\alpha_{440-870}$ , with extreme values ranging from  $<0.2$  to  $>1.5$ . The 2-month average  $\alpha_{440-870}$  ranged from 0.77 over Arabian Gulf island sites, to 0.64 at coastal sites, and 0.50–0.57 at inland desert sites. The average fine mode fraction (as computed from the O'Neill et al. algorithm) corresponding to these  $\alpha_{440-870}$  values was  $\sim 48\%$  on the Gulf island sites versus  $\sim 35\%$  in the inland desert sites. The higher  $\alpha_{440-870}$  over Gulf sites results from the majority of the petroleum extraction and processing industries being located on islands, offshore platforms, and coastal locations, while the primary sources of the coarse mode aerosols are in the inland desert regions.

[50] 2. Two sites (Umm Al Quwain and Dhadnah) located at nearly the same latitude and 70 km apart east–west, but separated by a mountain range, were compared. One site

was located on the Arabian Gulf coast while the other was near the Gulf of Oman. Time matched observations showed that there was high correlation in both  $\tau_{a500}$  ( $r^2 = 0.61$ ) and  $\alpha_{440-870}$  ( $r^2 = 0.74$ ), thereby suggesting that in most cases the Al Hajar mountain range does not act as a barrier to aerosol advection. Comparison of  $\tau_{a500}$  at two other sites located 28 km apart but differing in altitude by 800 m showed that on average  $\sim 75\%$  of the total column aerosol loading was located above the lowest 800-m layer. Since the mountain range separating the sites on the Arabian Gulf and the Gulf of Oman is of a similar altitude, this suggests that the aerosol layer is much thicker than the mountain range height and thus there is relatively little blockage by the mountains.

[51] 3. Average diurnal variability of  $\tau_{a500}$  varied widely between sites, with the largest diurnal changes occurring at some coastal sites and island sites (probably associated with land breeze/sea breeze circulation) however one inland site near the mountains exhibited a large increase in the late afternoon, possibly due to the influence of haboob winds associated with thunderstorms. The diurnal variation of  $\alpha_{440-870}$  was also largest for some coastal and island sites, again likely due to land breeze/sea breeze circulation.

[52] 4. Aerosol optical depth increased as total column water vapor increased at both inland desert sites and coastal sites, with correlation coefficients ranging from  $\sim 0.45$  to  $\sim 0.65$ . This trend occurs for both fine and coarse mode dominated aerosol cases suggesting that major aerosol sources are associated with transport over the humid Gulf and also possibly from haboob-generated dust associated with thunderstorm activity that occurs when column water vapor is high.

[53] 5. Version 2 almucantar retrievals of aerosol single scattering albedo show significant differences compared to version 1 retrievals. These differences are likely due primarily to more accurate estimates of surface reflectance. For example, in version 1 the  $\omega_0$  for dust aerosol over a Gulf island site and over a bright desert site differ significantly ( $\sim 0.03$ ) and show little spectral variation. However, in version 2 the retrievals for these same scans show very good agreement (differences  $<0.01$ ) and also significant increases in absorption at 440 nm, which is typical of dust with iron content. These comparisons suggest significant improvement in the version 2 retrievals of absorption.

[54] 6. During pollution events when fine mode particles dominated ( $\alpha_{440-870} > 1$ ), the average retrieved peak volume fine mode particle radius was larger over a Gulf island site ( $\sim 0.160 \mu\text{m}$ ) than over a desert site ( $\sim 0.135 \mu\text{m}$ ), which was probably due to hygroscopic growth in the high RH marine environment. Coincident with the particle growth at the marine site is higher single scattering albedo over the Gulf for the pollution dominated events ( $\sim 0.03$ ) than at the desert site.

[55] 7. At an inland desert site (Hamim), the single scattering albedo at 440 nm remains relatively constant (within  $\sim 0.01$ ) as a function of Angstrom exponent since both fine and coarse mode particles are absorbing at this wavelength. At longer wavelengths (675 to 1020 nm), however, the dust is much less absorbing than the pollution, resulting in differences of  $\sim 0.04$ – $0.05$  between dust cases with  $\alpha_{440-870} < 0.4$  and pollution cases with  $\alpha_{440-870} > 1.0$ . At a Gulf island site (Sir Bu Nuair) there is less contrast in

the  $\omega_0$  at the longer wavelengths since the pollution aerosol is less absorbing than over the desert.

[56] 8. At the Gulf coastal site of MAARCO from 27 August to 30 September 2004 the aerosol single scattering albedo retrieved from AERONET almucantar scans averaged  $\sim 0.03$  higher in the late afternoon than in the early morning. This is consistent with but less than the  $\sim 0.05$  greater afternoon  $\omega_0$  measured in situ at the surface at this same site and times. This diurnal change is likely related to the land breeze/sea breeze diurnal cycle, with more absorbing pollution aerosol building up over night and aerosol of a more weakly absorbing nature being advected inland during the day with the sea breeze. However, another AERONET coastal site in a more rural location does not show any diurnal variation in retrieved  $\omega_0$  thus suggesting that this dynamic may result from MAARCO being located in a relatively highly industrialized section of the Gulf coast.

[57] **Acknowledgments.** This project was supported by Michael D. King, NASA EOS project office. We thank the staff at the United Arab Emirates Department of Water Resources, directed by Abdulla Al Mangosho, for extensive assistance in all aspects of this field campaign. Steve Braccardo (University of Witwatersrand, Johannesburg, South Africa) was responsible for the UAE<sup>2</sup> field campaign project management. We also thank the anonymous reviewers for comments that resulted in improvements in the paper.

## References

- Anderson, T. L., S. J. Masonis, D. S. Covert, N. C. Ahlquist, S. G. Howell, A. D. Clarke, and C. S. McNaughton (2003), Variability of aerosol optical properties derived from in situ aircraft measurements during ACE-Asia, *J. Geophys. Res.*, **108**(D23), 8647, doi:10.1029/2002JD003247.
- Arimoto, R., et al. (2006), Characterization of Asian dust during ACE-Asia, *Global Planet. Change*, **52**, 23–56.
- Bergstrom, R. W., P. B. Russell, and P. Hignett (2002), Wavelength dependence of the absorption of black carbon particles: Predictions and results from the TARFOX experiment and implications for the aerosol single scattering albedo, *J. Atmos. Sci.*, **59**, 567–577.
- Carrico, C. M., P. Kus, M. J. Rood, P. K. Quinn, and T. S. Bates (2003), Mixtures of pollution, dust, sea salt, and volcanic aerosol during ACE-Asia: Radiative properties as a function of relative humidity, *J. Geophys. Res.*, **108**(D23), 8650, doi:10.1029/2003JD003405.
- Cox, C., and W. Munk (1954), The measurements of the roughness of the sea surface from photographs of the Sun's glitter, *J. Opt. Soc. Am.*, **44**, 838–850.
- Dubovik, O., and M. D. King (2000), A flexible inversion algorithm for the retrieval of aerosol optical properties from Sun and sky radiance measurements, *J. Geophys. Res.*, **105**, 20,673–20,696.
- Dubovik, O., A. Smirnov, B. N. Holben, M. D. King, Y. J. Kaufman, T. F. Eck, and I. Slutsker (2000), Accuracy assessments of aerosol optical properties retrieved from AERONET Sun and sky-radiance measurements, *J. Geophys. Res.*, **105**, 9791–9806.
- Dubovik, O., et al. (2006), Application of spheroid models to account for aerosol particle nonsphericity in remote sensing of desert dust, *J. Geophys. Res.*, **111**, D11208, doi:10.1029/2005JD006619.
- Eck, T. F., B. N. Holben, J. S. Reid, O. Dubovik, A. Smirnov, N. T. O'Neill, I. Slutsker, and S. Kinne (1999), Wavelength dependence of the optical depth of biomass burning, urban, and desert dust aerosols, *J. Geophys. Res.*, **104**, 31,333–31,349.
- Eck, T. F., B. N. Holben, D. E. Ward, O. Dubovik, J. S. Reid, A. Smirnov, M. M. Mukelabai, N. C. Hsu, N. T. O'Neill, and I. Slutsker (2001), Characterization of the optical properties of biomass burning aerosols in Zambia during the 1997 ZIBBEE Field Campaign, *J. Geophys. Res.*, **106**, 3425–3448.
- Eck, T. F., B. N. Holben, J. S. Reid, N. T. O'Neill, J. S. Schafer, O. Dubovik, A. Smirnov, M. A. Yamasoe, and P. Artaxo (2003), High aerosol optical depth biomass burning events: A comparison of optical properties for different source regions, *Geophys. Res. Lett.*, **30**(20), 2035, doi:10.1029/2003GL017861.
- Eck, T. F., et al. (2005), Columnar aerosol optical properties at AERONET sites in central eastern Asia and aerosol transport to the tropical mid-Pacific, *J. Geophys. Res.*, **110**, D06202, doi:10.1029/2004JD005274.
- Gomes, L., G. Bergametti, G. Coudé-Gaussen, and P. Rognon (1990), Submicron desert dusts: A sandblasting process, *J. Geophys. Res.*, **95**, 13,927–13,935.
- Holben, B. N., et al. (1998), AERONET—A federated instrument network and data archive for aerosol characterization, *Remote Sens. Environ.*, **66**, 1–16.
- Holben, B. N., T. F. Eck, I. Slutsker, A. Smirnov, A. Sinyuk, J. Schafer, D. Giles, and O. Dubovik (2006), AERONET's version 2.0 quality assurance criteria, Remote Sensing of Atmosphere and Clouds, *Proc. SPIE Int. Soc. Opt. Eng.*, **6408**, 64080Q, doi:10.1117/12.706524.
- Kalnay, E., et al. (1996), The NCEP/NCAR reanalysis 40-year project, *Bull. Am. Meteorol. Soc.*, **77**, 437–471.
- Li-Jones, X., H. B. Maring, and J. M. Prospero (1998), Effect of relative humidity on light scattering by mineral dust aerosol as measured in the marine boundary layer over the tropical Atlantic Ocean, *J. Geophys. Res.*, **103**, 31,113–31,122.
- Lucht, W., and J. L. Roujean (2000), Consideration in parametric modeling of BRDF and albedo from multi-angular satellite sensors observations, *Remote Sens. Rev.*, **18**, 343–379.
- Miller, S. D., A. P. Kuciauskas, M. Liu, Q. Ji, J. S. Reid, D. W. Breed, and A. Walker (2008), Haboob dust storms of the southern Arabian Peninsula, *J. Geophys. Res.*, doi:10.1029/2007JD008550, in press.
- Moody, E. G., M. D. King, S. Platnik, C. B. Schaaf, and F. Gao (2005), Spatially complete global spectral surface albedos: Value-added datasets derived from terra MODIS land products, *IEEE Trans. Geosci. Remote Sens.*, **43**, 144–158.
- O'Neill, N. T., T. F. Eck, B. N. Holben, A. Smirnov, O. Dubovik, and A. Royer (2001), Bimodal size distribution influences on the variation of Angstrom derivatives in spectral and optical depth space, *J. Geophys. Res.*, **106**, 9787–9806.
- O'Neill, N. T., T. F. Eck, B. N. Holben, A. Smirnov, A. Royer, and Z. Li (2002), Optical properties of boreal forest fire smoke derived from Sun photometry, *J. Geophys. Res.*, **107**(D11), 4125, doi:10.1029/2001JD000877.
- O'Neill, N. T., T. F. Eck, A. Smirnov, B. N. Holben, and S. Thulasiraman (2003), Spectral discrimination of coarse and fine mode optical depth, *J. Geophys. Res.*, **108**(D17), 4559, doi:10.1029/2002JD002975.
- O'Neill, N. T., T. F. Eck, J. S. Reid, A. Smirnov, and O. Pancrati (2008), Coarse mode optical information retrievable using VIS to SWIR Sun photometry: Application to UAE2 data, *J. Geophys. Res.*, doi:10.1029/2007JD009052, in press.
- Redemann, J., S. J. Masonis, B. Schmid, T. L. Anderson, P. B. Russell, J. M. Livingston, O. Dubovik, and A. D. Clarke (2003), Clear-column closure studies of aerosols and water vapor aboard the NCAR C-130 during ACE-Asia, 2001, *J. Geophys. Res.*, **108**(D23), 8655, doi:10.1029/2003JD003442.
- Reid, J. S., T. F. Eck, S. A. Christopher, P. V. Hobbs, and B. N. Holben (1999), Use of the Angstrom exponent to estimate the variability of optical and physical properties of aging smoke particles in Brazil, *J. Geophys. Res.*, **104**, 27,473–27,489.
- Reid, J. S., et al. (2003), Comparison of size and morphological measurements of coarse mode dust particles from Africa, *J. Geophys. Res.*, **108**(D19), 8593, doi:10.1029/2002JD002485.
- Remiszewska, J., P. J. Flatau, K. M. Markowicz, E. A. Reid, J. S. Reid, and M. L. Witek (2007), Modulation of the aerosol absorption and single-scattering albedo due to synoptic scale and sea breeze circulations: United Arab Emirates experiment perspective, *J. Geophys. Res.*, **112**, D05204, doi:10.1029/2006JD007139.
- Schmid, B., J. Michalsky, R. Halthore, M. Beauharnois, L. Harrison, J. Livingston, P. Russell, B. Holben, T. Eck, and A. Smirnov (1999), Comparison of aerosol optical depth from four solar radiometers during the fall 1997 ARM intensive observation period, *Geophys. Res. Lett.*, **26**, 2725–2728.
- Schmid, B., et al. (2003), Column closure studies of lower tropospheric aerosol and water vapor during ACE-Asia using airborne Sun photometer and airborne in situ and ship-based lidar measurements, *J. Geophys. Res.*, **108**(D23), 8656, doi:10.1029/2002JD003361.
- Sinyuk, A., et al. (2007), Simultaneous retrieval of aerosol and surface properties from a combination of AERONET and satellite, *Remote Sens. Environ.*, **107**, 90–108, doi:10.1016/j.rse.2006.07.022.
- Smirnov, A., B. N. Holben, T. F. Eck, O. Dubovik, and I. Slutsker (2000), Cloud screening and quality control algorithms for the AERONET data base, *Remote Sens. Environ.*, **73**, 337–349.
- Smirnov, A., B. N. Holben, T. F. Eck, I. Slutsker, B. Chatenet, and R. T. Pinker (2002a), Diurnal variability of aerosol optical depth observed at AERONET (Aerosol Robotic Network) sites, *Geophys. Res. Lett.*, **29**(23), 2115, doi:10.1029/2002GL016305.
- Smirnov, A., B. N. Holben, O. Dubovik, N. T. O'Neill, T. F. Eck, D. L. Westphal, A. K. Goroch, C. Pietras, and I. Slutsker (2002b), Atmo-

- spheric aerosol optical properties in the Persian Gulf, *J. Atmos. Sci.*, **59**, 620–634.
- Sokolik, I. N., and O. B. Toon (1999), Incorporation of mineralogical composition into models of the radiative properties of mineral aerosol from UV to IR wavelengths, *J. Geophys. Res.*, **104**, 9423–9444.
- Volten, H., O. Muñoz, E. Rol, J. F. de Haan, W. Vassen, J. W. Hovenier, K. Muinonen, and T. Nousiainen (2001), Scattering matrices of mineral aerosol particles at 441.6 nm and 632.8 nm, *J. Geophys. Res.*, **106**, 17,375–17,402.
- A. Al Mandoos and M. Ramzan Khan, Department of Atmospheric Studies, Ministry of Presidential Affairs, P.O. Box 4815, Abu Dhabi, United Arab Emirates.
- O. Dubovik, Laboratoire d'Optique Atmosphérique, CNRS Université de Lille 1, Bat P5 Cite scientifique, F-59655 Villeneuve d'Ascq Cedex, France.
- T. F. Eck, D. Giles, B. N. Holben, W. Newcomb, J. S. Schafer, A. Sinyuk, I. Slutsker, A. Smirnov, and M. Sorokine, NASA Goddard Space Flight Center, Code 614.4, Greenbelt, MD 20771, USA. (teck@ltpmail.gsfc.nasa.gov)
- Q. Ji and S.-C. Tsay, NASA Goddard Space Flight Center, Code 613.2, Greenbelt, MD 20771, USA.
- N. T. O'Neill, CARTEL, Université de Sherbrooke, Sherbrooke, QC, Canada J1K 2R1.
- E. A. Reid and J. S. Reid, Aerosol and Radiation Section, Marine Meteorology Division, Naval Research Laboratory, 7 Grace Hopper Avenue, Stop 2, Monterey, CA 93943-5502, USA.